

**MEASUREMENT UNCERTAINTY
ESTIMATION IN AMPEROMETRIC
DISSOLVED OXYGEN
CONCENTRATION MEASUREMENT**

LAURI JALUKSE



TARTU UNIVERSITY
PRESS

Department of Chemistry, University of Tartu, Estonia

Dissertation is accepted for the commencement of the Degree of Doctor of Philosophy in Chemistry on May 2th, 2007 by the Doctoral Committee of the Department of Chemistry, University of Tartu.

Supervisor: Professor Ivo Leito (PhD)

Opponents: Dr. Michal Máriássy, Slovak Institute of Metrology, Slovakia
Dr. Kaido Tammeveski, University of Tartu, Estonia

Commencement: 2:00 PM, June 29th, 2007, 2 Jakobi St., room 154

Publication of this dissertation is granted by University of Tartu

ISSN 1406–0299

ISBN 978–9949–11–632–4 (trükis)

ISBN 978–9949–11–633–1 (PDF)

Autoriõigus Lauri Jalukse, 2007

Tartu Ülikooli Kirjastus

www.tyk.ee

Tellimuse nr 197

CONTENTS

1. INTRODUCTION.....	8
2. THEORY.....	10
3. DERIVING THE EQUATIONS FOR DEFINING THE MATHEMATICAL MODEL	11
4. OXYGEN CONCENTRATION IN AIR-SATURATED DISTILLED WATER	16
5. DEFINING THE INITIAL MATHEMATICAL MODEL	17
6. EXPERIMENTAL	18
6.1. Reagents.....	18
6.2. Instrumentation	18
6.3. Detailed technical information of the Instrument I.....	19
6.4. Detailed technical information of the Instrument II	19
6.5. Calibration of the instruments.....	20
7. UNCERTAINTY SOURCES	23
7.1. Explicit Uncertainty Sources	23
7.2. Implicit Uncertainty Sources	25
7.3. Quantifying the Uncertainty Components	27
8. THE FINAL MATHEMATICAL MODEL.....	33
9. RESULTS AND DISCUSSION	34
10. DISSOLVED OXYGEN <i>IN SITU</i> INTERLABORATORY COMPARISON	42
10.1. Description of the <i>in situ</i> ILC Apparatus and Measurement Conditions	42
10.2. Reference Values and their Uncertainties	43
10.3. Results of the Instrument I Participating to the <i>in situ</i> ILC.....	43
SUMMARY	45
SUMMARY IN ESTONIAN	46
REFERENCES.....	47
ACKNOWLEDGEMENTS	49
APPENDIX 1	50
APPENDIX 2	54
APPENDIX 3	64
PUBLICATIONS	75

LIST OF ORIGINAL PUBLICATIONS

This thesis consists of three articles listed below and a review. The articles are referred in the text by Roman numerals I–III. The review summarizes and supplements the articles.

- I. **L. Jalukse**, I. Leito, A. Mashirin and T. Tenno, Estimation of uncertainty in electrochemical amperometric measurement of dissolved oxygen concentration. *Accreditation and Quality Assurance* 2004, 9, 340–348, <http://dx.doi.org/10.1007/s00769-004-0783-4>
- II. **L. Jalukse** and I. Leito, Model-based measurement uncertainty estimation in amperometric dissolved oxygen concentration measurement. *Measurement Science and Technology* 2007, 18, 1877–1886, <http://dx.doi.org/10.1088/0957-0233/18/7/013>
- III. **L. Jalukse**, V. Vabson and I. Leito, In situ interlaboratory comparisons for dissolved oxygen concentration and pH. *Accreditation and Quality Assurance* 2006, 10, 562–564, <http://dx.doi.org/10.1007/s00769-005-0058-8>

Paper I: One of the two main contributors to writing the text. Performed all calculations and part of the experimental work.

Paper II: Main person responsible for planning and writing. Performed all experimental work.

Paper III: Main person responsible for planning and writing. Performed all experimental work.

ABBREVIATIONS

DO	Dissolved oxygen
ILC	Interlaboratory Comparison
ISO	International Organization for Standardization
GUM	The Guide to the Expression of Uncertainty in Measurement

1. INTRODUCTION

Dissolved oxygen (DO) concentration measurement is a widely applied measurement in many industrial and laboratory applications (environmental, wastewater treatment plants, medical etc).

The most common way of DO concentration measurement is using amperometric sensors. The theory of operation and practical usage of amperometric oxygen sensors [1, 2] as well as the reliability of DO measurements [3–10] has been discussed extensively in literature including several excellent reviews. It is now widely recognized that uncertainty forms an intrinsic part of a measurement result. Uncertainty estimates based on different assumptions and estimation schemes have been given for DO measurement in literature [1–9]. The measurement uncertainty of DO measurement has mostly been found between 1% and 3% (relative) provided the DO sensor is in good order and the calibration is performed correctly [3–10]. In spite of the extensive literature on DO concentration measurement, no convenient practically applicable procedure for estimation of uncertainty of DO concentration measurement with identification and quantification of individual uncertainty sources has been available. This procedure would be of interest to a large number of analysis laboratories. It would enable them to take into account changes in experimental conditions and predict the behaviour of the measurement system under different conditions.

The main goals of this work were the following:

- (1) To investigate and quantitatively evaluate the uncertainty sources of amperometric DO measurement instruments of galvanic type.
- (2) To develop a model-based uncertainty estimation procedure for DO measurement instruments of the galvanic type.
- (3) To apply the uncertainty budgeting to two DO instruments and to explore the structures of the uncertainty budgets depending on the design of the instruments as well as on the experimental conditions [II].
- (4) To draw, based on the uncertainty budgets, a set of conclusions and recommendations for the design of amperometric DO measurement instruments.

The ISO GUM approach [11, 12] is used for uncertainty estimation. The work is based on a detailed model of amperometric DO measuring instruments.

For a routine analysis laboratory participation to interlaboratory comparison schemes is the main (and often the only) possibility to ensure and improve the quality of measurement results [13]. Dissolved oxygen is an unstable analyte. Thus preparation of reference solutions that are stable for extended periods of time is complicated or outright impossible. This complicates the standardization of the measurement and organization of interlaboratory comparisons [14].

In situ interlaboratory comparisons are intercomparison measurements, where all the participants (with their technical equipment and using their own competence) are measuring the same sample at the same time, on the same site. Therefore, an additional goal of this work was to develop and implement at University of Tartu a scheme for *in situ* interlaboratory comparison measurements of dissolved oxygen concentration.

2. THEORY

An amperometric measuring instrument for measurement of dissolved oxygen (DO) concentration consists of the DO sensor and the meter (the electronic control unit) [15, 16, 17 and 18]. The DO sensor (see figure 1) consists of the electrode system (cathode and anode), the electrolyte solution and the polymeric membrane. Oxygen passes through the membrane, which is impermeable to ionic salts [15]. The DO sensor has a built-in temperature sensor for measuring the solution and membrane temperature, an important parameter for converting the output current of the sensor into oxygen concentration [10, 15].

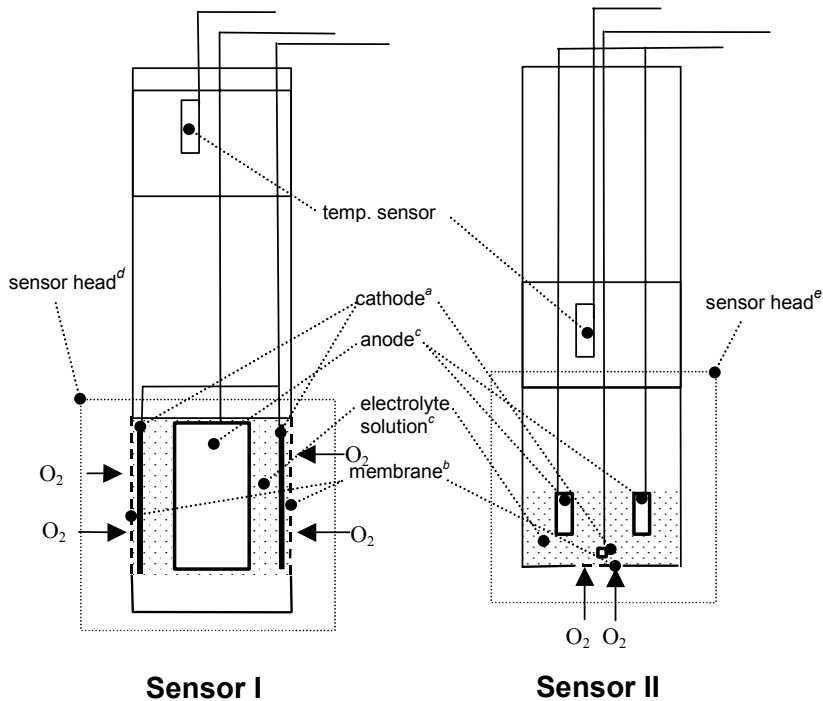


Figure 1. Schematic Presentation of the Galvanic DO Sensors.

^a Sensor I has macro Cr/Ni alloy cathode with area 5.265 cm², Sensor II has cathode area 0.0057 cm²

^b Sensor I has polypropylene (PP) side-membrane with thickness 25 μm, Sensor II has fluoroethylene-propylene (FEP) end membrane with thickness 13 μm

^c Both sensors have the same electrolyte solution and the anode material: KOH solution and Pb, respectively

^d Sensor head I include cathode, anode, electrolyte and membrane is replaced as one piece [16]

^e Sensor head II include cathode, anode, electrolyte and membrane. Cathode and anode can not be replaced but can be cleaned. Membrane and electrolyte can be replaced [17].

3. DERIVING THE EQUATIONS FOR DEFINING THE MATHEMATICAL MODEL

In the gas phase the sensor current is proportional to the partial pressure of oxygen at the surface of the membrane:

$$J_{\text{O}_2\text{-air}} = n \cdot F \cdot S \cdot \left(\frac{l_{\text{me}}}{P_{\text{me}}} \right)^{-1} \cdot p_{\text{O}_2} \quad (1)$$

where p_{O_2} [Pa] is the measured oxygen partial pressure, $J_{\text{O}_2\text{-air}}$ [A] is the sensor current, n [unitless] is the number of electrons participating in the cathode reaction, F [C mol⁻¹] is the Faraday constant, S [cm²] is the diffusion surface area (cathode area covered by the membrane) of the sensor, l_{me} [cm] is the thickness of the compound diffusion layer (sum of membrane thickness and electrolyte solution layer thickness), P_{me} [mol cm⁻¹ s⁻¹ Pa(O₂)⁻¹] is the oxygen permeability coefficient of the compound diffusion layer formed by the membrane and the electrolyte solution at the measurement temperature.

The permeability of the membrane and electrolyte solution to oxygen varies with temperature. The dependence is described by the eq 2 [3, 19]:

$$P_{\text{me}} = P_{\text{me}}^0 \cdot e^{\frac{E_{\text{me}}}{R \cdot T}} \quad (2)$$

where P_{me}^0 [mol (cm s Pa(O₂))⁻¹] is the standard permeability pre-exponential coefficient, which is the product of the distribution and diffusion pre-exponential coefficients (henceforth: standard permeability pre-exponential coefficient) [10]. Detailed description of the calculations of P_{me}^0 is available in appendix 1. E_{me} [J mol⁻¹] is the activation energy of the combined processes of oxygen permeation through the compound diffusion layer (which consists of the membrane and the electrolyte solution) to the cathode [10] (henceforth: activation energy of diffusion), T [K] is the temperature.

In this treatment we assume that the diffusion layer (having thickness l_{me}) is a compound layer consisting of the polymeric membrane (with thickness l_{m}) and the inner electrolyte solution layer (with thickness l_{e}). The ratio of the compound layer thickness to its permeability can be treated as the resistance of the layer to diffusion of oxygen and can be expressed as sum of similar resistances of the two sub-layers as follows:

$$\frac{l_{\text{me}}}{P_{\text{me}}} = \frac{l_{\text{m}}}{P_{\text{m}}} + \frac{l_{\text{e}}}{P_{\text{e}}} \quad (3)$$

The situation is analogous to the electric resistance of serially connected resistors. The sensor does not measure directly the analytical concentration of DO in water but the effective concentration of DO [10]. The reason why results of DO concentration measurements can in most cases be presented as analytical concentrations is that calibration is usually carried out in a medium where the activity coefficient of oxygen is the same as in the medium where the measurement is carried out.

The effective concentration can be characterized by the energy density of oxygen dissolution in water with the unit J m^{-3} . The concept of energy density enables to unify the metrological basis for measurement of DO content in both gaseous and liquid phases [19]. The energy density unit is equivalent to the unit of pressure Pa. Therefore it is justified to measure the solubility as an effective quantity – energy density, which for the gas phase is equivalent to the partial pressure of oxygen [19].

The partial pressure of oxygen, the partition coefficient of oxygen between water and the gas phase – the Henry's constant – and the concentration of DO are linked by the Henry's law [10, 19]:

$$p_{\text{O}_2} = K_h \cdot C_{\text{O}_2} \quad (4)$$

K_h depends on temperature according to the following equation [10]:

$$K_h = K_h^0 \cdot e^{\frac{H}{R \cdot T}} \quad (5)$$

where, K_h^0 [$\text{Pa}(\text{O}_2) \text{ dm}^3 \text{ mg}^{-1}$] is the oxygen partition pre-exponential coefficient [10] (henceforth: standard partition pre-exponential coefficient), H [J mol^{-1}] is the oxygen dissolution enthalpy in water [10]. The value of H has been found using solubility data from literature [15, 20]. Detailed description of the calculations of K_h^0 and H can be found in appendix 1. The equations 1 and 4 can be united to give:

$$J_{\text{O}_2_water} = n \cdot F \cdot S \cdot \frac{P_{\text{sme}}}{l_{\text{sme}}} \cdot K_h \cdot C_{\text{O}_2} \quad (6)$$

When measurement is carried out in water then an additional diffusion layer is formed by the stagnant solution layer between the membrane and the bulk solution. The thickness l_s of the stagnant solution layer depends on the surface roughness of the membrane and stirring speed [18, 21]. The overall permeability of the compound layer can now be described by the following equation:

$$\frac{l_{\text{sme}}}{P_{\text{sme}}} = \frac{l_s}{P_s} + \frac{l_m}{P_m} + \frac{l_e}{P_e} \quad (7)$$

In water P_{sme} is related to diffusion of oxygen through the compound diffusion layer consisting of the stagnant solution, membrane and the electrolyte solution. This leads to somewhat lower current when measuring in the liquid phase compared to the gas phase with equal energy density of oxygen. The higher current in the gas phase compared to the liquid phase under the same conditions (due to the additional layer) can be compensated by a correction factor g . Equations 1, 3, 6 and 7 can be united to give:

$$g = \frac{J_{O_2_air}}{J_{O_2_water}} = 1 + \frac{\frac{l_s}{P_s}}{\frac{l_m}{P_m} + \frac{l_e}{P_e}} \quad (8)$$

The g factor is found empirically as a rule. The value of the g factor depends on the thickness of the additional layer. The layer thickness depends on surface roughness of the membrane and the stirring speed [21]. P_{sme} varies with temperature as described by eq 9:

$$P_{\text{sme}} = P_{\text{sme}}^0 \cdot e^{\frac{E_{\text{sme}}}{R \cdot T}} \quad (9)$$

where P_{sme}^0 [mol (cm s Pa(O₂))⁻¹] is the standard permeability pre-exponential coefficient, which is the product of the distribution and diffusion pre-exponential coefficients [10] (henceforth: standard permeability pre-exponential coefficient). E_{sme} [J mol⁻¹] is the activation energy of the combined processes of oxygen permeation (henceforth: activation energy of diffusion) through the compound diffusion layer (which consists of the measured solution, membrane and the electrolyte solution) to the cathode [10], T [K] is the temperature. E_{sme} is determined by the sensor design (first of all by the membrane material). Detailed description of the calculations of P_{sme}^0 and E_{sme} can be found in appendix 1.

Uniting to equations 5, 6 and 9 the sensor current in the measured solution can be expressed as follows:

$$J_{\text{meas}} = n \cdot F \cdot S \cdot \frac{1}{l_{\text{sme_meas}}} \cdot P_{\text{me}}^0 \cdot K_{\text{h}}^0 \cdot e^{\frac{E_{\text{sme}} + H}{R \cdot T_{\text{meas}}}} \cdot C_{\text{meas}} \quad (10)$$

where T_{meas} [K] is the measurement temperature, $l_{\text{sme_meas}}$ [cm] is the thickness of the diffusion layer (stagnant solution layer, membrane and electrolyte solution) during the measurement, C_{meas} [mg dm⁻³] is the concentration of oxygen in the measured solution (water) at the measurement temperature. Calibration is carried out in distilled water saturated with air. During calibration the following equation holds:

$$J_{\text{cal_water}} = n \cdot F \cdot S \cdot \frac{1}{l_{\text{sme_cal}}} \cdot P_{\text{me}}^0 \cdot K_{\text{h}}^0 \cdot e^{\frac{E_{\text{sme}} + H}{R \cdot T_{\text{cal}}}} \cdot C_{\text{sat_cal_water}} \cdot W \quad (11)$$

where T_{cal} [K] is the calibration temperature, $l_{\text{me_cal}}$ [cm] is the thickness of the diffusion layer (stagnant solution layer, membrane and electrolyte solution) during the calibration, $C_{\text{sat_cal_water}}$ [mg dm⁻³] is the concentration of oxygen in air-saturated distilled water at the calibration temperature. W is the pressure correction factor [unitless] (see section 4). Detailed description of finding the value $C_{\text{sat_cal_water}}$ is presented in section 4.

Good linearity of amperometric sensors is well known [1, 10, 15] and linear calibration functions are used in DO measurement instruments. Based on the linearity of the sensor response the concentration of DO in water during measurement can be expressed as follows:

$$C_{\text{meas}} = \frac{J_{\text{meas}}}{J_{\text{cal_water}}} \cdot C_{\text{sat_cal_water}} \quad (12)$$

If calibration is carried out in air (as frequently advised by the instrument manufacturers) then in order to obtain correct DO results in water the additional diffusion layer is taken into account using the empirical g value and the sensor current based on eq 8 can be expressed as follows:

$$C_{\text{meas}} = \frac{J_{\text{meas}}}{J_{\text{cal_air}}} \cdot C_{\text{sat_cal_water}} \cdot g \quad (13)$$

The output current of the sensor is caused not only by the flux of oxygen from the measured solution to the cathode. A small portion of the current is caused by other electrochemical reactions on the electrodes, parasitic currents from electrical connections, residual current in the sensor materials and dissolved oxygen in the electrolyte solution [10, 22, 23]. This additional current is called zero current and is denoted as J_0 below. We arrive at the following:

$$J_{\text{meas_output}} = J_{\text{meas}} + J_0 \quad (14)$$

$$J_{\text{cal_output_water}} = J_{\text{cal_water}} + J_0 \quad (15)$$

$$J_{\text{cal_output_air}} = J_{\text{cal_air}} + J_0 \quad (16)$$

Combining the above equations we get:

$$C_{\text{meas}} = \frac{J_{\text{meas_output}} - J_0}{J_{\text{cal_output}} - J_0} \cdot C_{\text{sat_cal_water}} \quad (17)$$

In almost all commercial DO measurement instruments two-point calibration is used. One of the points is the zero point of the sensor. At the zero point, the sensor signal obtained in the absence of oxygen lies below the resolution of the sensor [18]. The second point of the calibration line is normally the point corresponding to the saturation concentration at the calibration temperature.

4. OXYGEN CONCENTRATION IN AIR-SATURATED DISTILLED WATER

$C_{\text{sat_cal_water}}$ [mg dm⁻³] is normally found using one of the various available empirical equations [4, 20]. We use the values that are used in the ISO 5814 standard [15] based on equation from Benson and Krause [24]:

$$C_{\text{sat_cal_water}} = \exp \left(A_1 + \frac{A_2}{T_{\text{cal}}} + \frac{A_3}{(T_{\text{cal}})^2} + \frac{A_4}{(T_{\text{cal}})^3} + \frac{A_5}{(T_{\text{cal}})^4} \right) \quad (18)$$

where A_1, A_2, A_3, A_4 and A_5 are constants [20, 24]. This equation has been found by Mortimer [20] to be one of the best available. In eq 11 W is the pressure correction factor [15]:

$$W = \frac{p_{\text{cal}} - p_{\text{H}_2\text{O_cal}}}{p_{\text{n}} - p_{\text{H}_2\text{O_100\%}}} \quad (19)$$

where p_{cal} [Pa] is atmospheric pressure at calibration conditions, $p_{\text{H}_2\text{O_cal}}$ [Pa] is the real content of H₂O in air (found experimentally during aeration in calibration conditions), p_{n} [Pa] is atmospheric pressure at standard conditions and $p_{\text{H}_2\text{O_100\%}}$ [Pa] is the water vapor pressure at 100% relative humidity. It is found according to equation 20 [20]:

$$p_{\text{H}_2\text{O_100\%}} = p_{\text{n}} \cdot \exp \left(B_1 + \frac{B_2}{T_{\text{cal}}} + \frac{B_3}{(T_{\text{cal}})^2} \right) \quad (20)$$

where B_1, B_2 and B_3 are empirical constants.

5. DEFINING THE INITIAL MATHEMATICAL MODEL

If calibration was carried out in distilled water then based on equations 10–12, 14 and 15 DO concentration in the measured solution is found as:

$$C_{\text{meas}} = \frac{J_{\text{meas}} \cdot l_{\text{sme_meas}}}{J_{\text{cal_water}} \cdot l_{\text{sme_cal}}} \cdot e^{\frac{E_{\text{sme}} + H}{R} \left(\frac{1}{T_{\text{cal}}} - \frac{1}{T_{\text{meas}}} \right)} \cdot W \cdot C_{\text{sat_cal_water}} \quad (21)$$

where C_{meas} [mg dm^{-3}] is the concentration of oxygen in the measured solution (water) at the measurement temperature, J_{meas} [A] is the sensor current during measurement, $l_{\text{sme_meas}}$ [cm] is the thickness of the compound diffusion layer (consisting of the stagnant solution layer, membrane and electrolyte solution) during the measurement, $J_{\text{cal_water}}$ [A] is the sensor current during calibration, $l_{\text{sme_cal}}$ [cm] is the thickness of the compound diffusion layer (see the section 3) during calibration, E_{sme} [J mol^{-1}] is the activation energy of the combined processes of oxygen permeation through the compound diffusion layer to the cathode [10] (henceforth: activation energy of diffusion), H [J mol^{-1}] is the oxygen dissolution enthalpy in water [10], T_{meas} [K] is the measurement temperature, T_{cal} [K] is the calibration temperature, W is the pressure correction factor [15], $C_{\text{sat_cal_water}}$ is the concentration of oxygen in air-saturated distilled water at calibration temperature [mg dm^{-3}] [15, 20]. If the calibration was carried out in air then based on equations 10, 11, 13, 14 and 16. DO concentration in the measured solution is found as:

$$C_{\text{meas}} = \frac{J_{\text{meas}} \cdot l_{\text{sme_meas}}}{J_{\text{cal_air}} \cdot l_{\text{sme_cal}}} \cdot e^{\frac{E_{\text{sme}} + H}{R} \left(\frac{1}{T_{\text{cal}}} - \frac{1}{T_{\text{meas}}} \right)} \cdot W \cdot C_{\text{sat_cal_water}} \cdot g \quad (22)$$

$J_{\text{cal_air}}$ [A] is the sensor current during calibration in air, g [unitless] is the correction factor for air calibration (see the eq 8). Equations 21 and 22 with the supporting equations are our initial mathematical models.

6. EXPERIMENTAL

6.1. Reagents

Anhydrous sodium sulfite (Na_2SO_3) (Reakhim, Analytically pure). Cobalt(II)chloride hexahydrate ($\text{CoCl}_2 \cdot 6\text{H}_2\text{O}$) (Reakhim, Analytically pure). Alkaline Electrolyte Solution for Galvanic Oxygen Probes, Cleaning Solution for Galvanic Oxygen Probes (Wissenschaftliche-Technische Werkstätten GmbH, Germany, below WTW). Aqueous solutions were prepared with distilled water.

6.2. Instrumentation

The instruments were Marvet Junior 2000 (below instrument I) with HELOX-13 sensor (below sensor I) [16] and WTW OXI340i (below instrument II) with CelloX 325 sensor (below sensor II) [17, 18]. The sensors are schematically presented in figure 1. These instruments work according to the same principle but they do have two important differences that have their consequences from metrology point of view. Firstly, the sensor I has a Cr/Ni alloy cathode with large area 5.265 cm^2 and side-membrane, while the sensor II has around 1000 smaller gold cathode (area 0.0057 cm^2) and end-membrane. Secondly, the sensor I has polypropylene (PP) membrane with thickness $25 \text{ }\mu\text{m}$, while the sensor II has fluoroethylene-propylene (FEP) membrane with thickness $13 \text{ }\mu\text{m}$. According to our results the permeability (or permeation rate) of the PP membrane is around three times lower than that of the FEP membrane. Detailed description of the membrane parameters can be found in appendix 1. The thicker is the membrane and the lower is its permeability the less is the sensor sensitive to stirring speed and changes of the electrolyte layer thickness and thus the more stable and rugged is the sensor [5]. However, with increasing stability the response time also increases. The electrolyte solution volume in sensors I and II is around 0.5 cm^3 and 0.7 cm^3 , respectively. Both types of sensors have the same electrolyte solution and anode material: KOH and Pb, respectively.

The manuals of the instruments provided to users by manufacturers [16, 17, 18] fulfill the minimum everyday requirements for obtaining DO measurement results. If slightly deeper coverage is desired, then the manual of the DO meter II with sensor II is clearly superior. In particular, the DO meter I with sensor I manual completely misses the following very important aspects: The influence of atmospheric pressure on the calibration, the difference in calibrating the instrument in air and in water (the g factor) and the necessary humidity conditions for calibrating in air. With both instruments the readings were

registered as follows: at temperatures 20 to 25°C readings were registered 3 min after immersion of the sensor; at temperatures 5 to 20°C readings were registered 5 min after immersion of the sensor.

6.3. Detailed technical information of the Instrument I

The instrument I, MJ2000 with sensor HELOX-13 (serial nr of DO meter: 03–0358; serial number of sensor: 385; manufacturer: Elke Sensor LLC, Estonia) has three-digit LCD display (one digit after the decimal point) and measuring range 0.0–20.0 mg dm⁻³. The accuracy of the temperature compensation in the full temperature range stated in the manual [16] is $\pm 2\%$ of the measured DO concentration value. The response time of the sensor at 20°C is about 1.5 to 2 minutes (at lower temperature the response time increases). Stirring that generates flow of water along the membrane of the sensor at velocity 5 cm s⁻¹ is sufficient. The temperature measurement capability and automatic temperature compensation covers the temperature range of –1...+30°C. The accuracy of temperature measurement for calibration and temperature correction is ± 0.2 K. If temperature measurement is carried out then additional uncertainty of ± 1 digit has to be taken into account. The sensor lifetime is around one year after which the sensor head can be replaced (see figure 1). The instrument I may be calibrated in air-saturated water or in air (the best results are obtained in air-saturated water) [16]. The instrument I does not have a built-in barometer. Atmospheric pressure was measured by an aneroid barometer BAMM-1 (Ser No 8858, manufactured in the former Soviet Union). Evaluated uncertainty is 200 Pa (k=2).

6.4. Detailed technical information of the Instrument II

The instrument II, Oxi340i with sensor CelloX 325 (serial nr of DO meter 04480005; serial number of sensor 04480255; manufacturer Wissenschaftliche-Technische Werkstätten GmbH, Germany) has four-digit LCD display (two digits after the decimal point) and measuring range 0.0–50 mg dm⁻³. The stated in manual accuracy in the full temperature range is 0.5% of the measured value at an ambient temperature of 5...30°C. The range for temperature measurement and automatic temperature compensation is –1...+40. The accuracy of temperature compensation in the whole temperature range is $< \pm 2\%$ of the measured DO concentration value. The stated accuracy of temperature measurement is ± 0.1 K. The atmospheric pressure correction is possible in the range of 500 ... 1100 mbar. The flow rate of water affects the measurement. The accuracy that can be obtained at different flow rates is according to the manual

the following: better than 10% at flow rates at and above 3 cm s^{-1} , better than 5% at flow rates at and above 10 cm s^{-1} and 1% at flow rates at and above $> 18 \text{ cm s}^{-1}$. The zero signal of the sensor is $< 0.1\%$ of the saturation value. The time needed for stabilization of the reading (response time) is specified as follows: 90% of the final value after $< 10 \text{ s}$, 95% of the final value after $< 16 \text{ s}$, 99% of the final value after $< 60 \text{ s}$. The long-term drift is approx. 3% per month under normal operating conditions. Useful lifetime of the sensor is minimum 6 months with one electrolyte fill. The instrument II may be calibrated in air-saturated water or in water vapor-saturated air (in the OxiCal®-SL vessel) [17].

6.5. Calibration of the instruments

According to literature the recommended calibration interval depends on the oxygen sensor used and ranges from two weeks for pocket instruments to 2–3 months for stationary oxygen sensors [16, 18]. The ISO 5814 standard [15] considers calibration in air as a valid option besides calibration in water. Air calibration is supported for both instruments: they may be calibrated in water saturated by air or in air saturated by water vapor.

6.5.1. Calibration in the air saturated water

Saturation calibration was performed in air saturated water (at 100% relative humidity) at constant temperature. The water was aerated until equilibrium was attained, that is the energy density of oxygen in air and in water was equal. Calibration was started after one hour from reaching the equilibrium. The calibration medium was created in thermostat CC2-K12 (Peter Huber Kältemaschinenbau GmbH, Germany). The thermostat provides temperature stability (according DIN 12876) of $\pm 0.03 \text{ K}$. Air saturated with water vapor was bubbled through the thermostat water. The level of saturation in the saturation vessel was measured using digital hygrometer Almemo 2290–8 with sensor ALMEMO FH A646 E1C (manufacturer AHLBORN Mess- und Regelungstechnik GmbH). The uncertainties of all relative humidity measurements are $\pm 10 \text{ \%RH}$ ($k=2$). CO_2 content in air was measured during calibration by Vaisala CARBOCAP® CO_2 Transmitter Series GMP 222 (SN: X0150001, manufactured by Vaisala, Finland). Evaluated uncertainty of the CO_2 concentration is $\pm 100 \text{ ppm}$ ($k=2$). The temperature of the measurement medium was measured by reference digital thermometer Chub-E4 (model nr 1529, serial No A44623, manufacturer Hart Scientific) with two Pt100 sensors. The uncertainties of all temperature measurements are $\pm 0.03^\circ\text{C}$ ($k=2$). Atmospheric pressure was measured during calibration by aneroid barometer BAMM-1 (Ser No 8858, manufactured in the former Soviet Union). The correctness of DO

concentration in the calibration solution (water) was determined by Winkler iodometric titration methods as reference method (according to ISO 5813:1983) [25].

6.5.2. Calibration in air saturated with water vapor

In the case of air-saturated water the energy density of oxygen in water is equal to its energy density in the gas phase (in air) in contact with water. Thus the output signal of the oxygen sensor in air is theoretically equal to the signal in air-saturated water at the same temperature under the condition that in water there is no stagnant solution layer formed between the membrane and the bulk solution. In reality the stagnant solution layer exists and this situation is taken into account by introducing the g factor (see eq 8). Before calibrating in air it is necessary to observe, that the surface of the sensor membrane is dry and the sensor is kept at constant temperature [16]. Calibration in air is accompanied by some inherent risks. The insufficient temperature equilibration between the body of the oxygen sensor and the ambient air is considered as one of the main sources of error. The evaporation heat of water from the wet sensor may cause temperature changes [26]. It is particularly important to take precautions after the sensor has been stored in the calibration vessel for an extended period of time and condensation droplets may have formed on the membrane [18]. It is necessary to take into account the correction factor g during calibration (see eq 13). The DO meter I does not take the g factor into account and its manual does not provide information on its magnitude. Therefore the g factor for this instrument was determined separately and was taken into account as a systematic uncertainty component if the instrument was calibrated in air (in a bottle containing pieces of moistened sponge). It was found that stabilization of the meter when calibrating in air took around 4 hours with sensor I. In the case of sensor II the magnitude of the g factor is 1.017 and the instrument takes it automatically into account when calibrating in air. Air calibration of the instrument II was carried out in the special OxiCal®-SL vessel. It was found that temperature stabilization took 2 hours. With both instruments calibration was done at 20°C (at 100% relative humidity).

6.5.3. Measurement of the zero current

The zero current of the sensors was measured in solution of sodium sulfite (1.00g of the salt per liter of water where 1 mg of cobalt chloride hexahydrate was added) [15]. The reading was taken two minutes after immersion of the sensor (see figure 2).

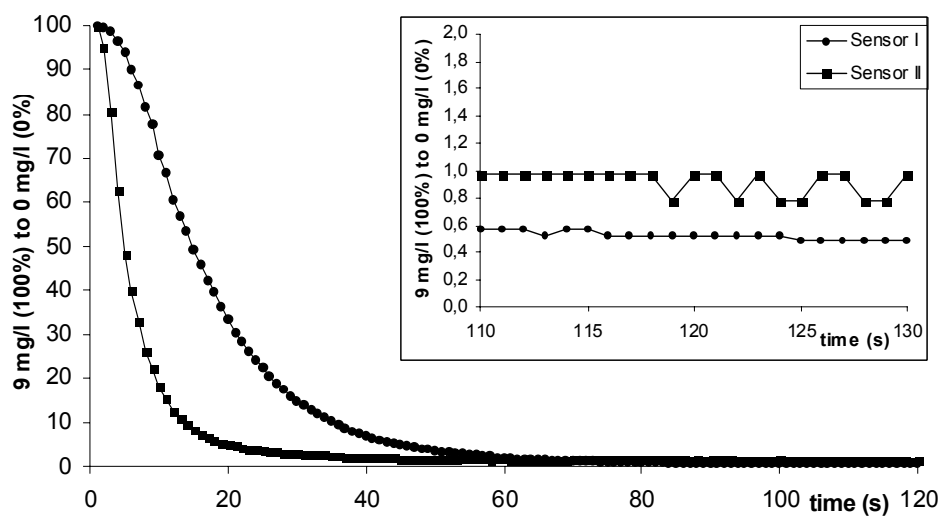


Figure 2. Determining the Sensors Zero Current Values after Two Minutes of Immersing in Solution of Sodium Sulfite (Water Free from Oxygen 0 mg dm^{-3} , Temperature 20°C).

7. UNCERTAINTY SOURCES

The cause and effect diagram to help to visualize the influence of the different uncertainty sources is presented in figure 3.

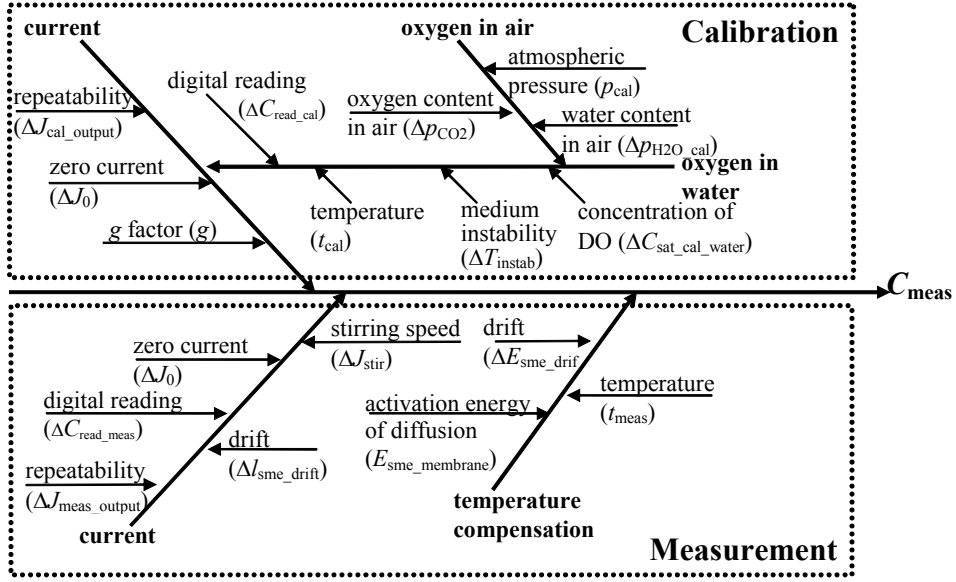


Figure 3. Cause and Effect Diagram for the Galvanic DO Instruments.

7.1. Explicit Uncertainty Sources

Currents $J_{\text{meas_output}}$ and $J_{\text{cal_output}}$. The following uncertainty sources are associated with these currents:

- (1) Repeatability of $J_{\text{meas_output}}$ and $J_{\text{cal_output}}$ measurements.
- (2) After immersing the sensor in the measured solution certain time has to pass until the current of the sensor reaches the stationary value. The time is proportional to the membrane thickness [27]. Modern sensors typically achieve stable response in 2 to 3 minutes [15]. We assume here, that the reading is taken only when it has stabilized and uncertainty due to the residual instability is included in the repeatability contribution.
- (3) Systematic deviations (bias) of the measured $J_{\text{meas_output}}$ value from the actual value. The systematic effects are due to drift of the properties of the sensor in time is due to different factors [3] and those will be taken into account separately (see below).

Thus the only uncertainty source taken into account directly in $J_{\text{meas_output}}$ and $J_{\text{cal_output}}$ is the repeatability.

The Zero Current J_0 . As said above the zero current is composed of two components: the true zero current (current that is present also under total absence of oxygen and is caused by different side-reactions [22, 23]) and the residual current (oxygen diffusing to the cathode from the electrolyte reservoir and the insulating body of the sensor [10]). In our treatment these two are handled jointly.

Thickness of the diffusion layer during measurement and calibration $l_{\text{sme_meas}}$ and $l_{\text{sme_cal}}$. In our model the drift of the response of the DO sensor is taken into account as the effective drift of the diffusion layer thickness, although in reality not all causes of drift lead to a change in the diffusion layer thickness. The main cause of drift is the instability of the distance between membrane and the cathode. Other causes are passivation of the cathode surface, leakage of the electrolyte, unstable reference potential, localized electrolyte concentration changes and gas bubbles in the electrolyte solution [6, 22]. The drift contribution was evaluated experimentally by monitoring the signal of the sensor during one month. The monitoring was carried out under two different sets of conditions leading to two different uncertainty contributions. The first set of conditions: new sensor (sensor I) or the electrolyte and membrane freshly replaced and the cathode and anode cleaned (sensor II). The second set of conditions: the sensor is at least one month old (sensor I) or at least one month has passed from the exchange of the electrolyte and membrane and cleaning of the cathode and anode (sensor II).

For uncertainty calculation we assume that the numerical values of $l_{\text{sme_cal}}$ and $l_{\text{sme_meas}}$ are the same and $u(l_{\text{sme_cal}}) = 0$ cm (because the status of the sensor during calibration is the reference status).

Atmospheric pressure during calibration p_{cal} . This uncertainty source is caused by the limited accuracy of the barometer used for measuring the atmospheric pressure and is taken into account as $u(p_{\text{cal}})$.

Pressure $p_{\text{H}_2\text{O_cal}}$. The sources of uncertainty taken into account by the input quantities of eq 19 are the imperfect saturation of the air with water vapor (determined experimentally) and the uncertainty arising from the imperfect fit of the mathematical model of the water vapor pressure at 100% relative humidity (eq 20) [4, 20]. We take this uncertainty into account as $u(p_{\text{H}_2\text{O_cal}})$.

Activation energy of diffusion E_{sme} . The following uncertainty sources are associated with E_{sme} :

- (1) The value of E_{sme} is pre-set in the DO measurement instrument and this value is not determined during calibration. The value preset by the manufacturer corresponds to the E_{me} of an average membrane [7]. Thus there is uncertainty due to the mismatch between the properties of the average membrane and the actual membrane of the sensor.
- (2) The exponential permeability function eq 9 does not exactly correspond to the real temperature dependence of the membrane permeability [1, 23, 28].

(3) The E_{sme} value is influenced by changes in properties of the membrane (slight deformation of the membrane, ageing, etc).

The first two uncertainty sources are jointly accounted for by $u(E_{\text{sme}})$. The third uncertainty source is taken into account by an additional parameter $\Delta E_{\text{sme_drift}}$. The uncertainty sources have been grouped according to how their contributions were estimated.

Temperature T_{meas} and T_{cal} . These uncertainties sources are caused by the limited accuracy of the temperature measurement during calibration and measurement. We take these uncertainties into account as $u(T_{\text{meas}})$ and $u(T_{\text{cal}})$.

Factor g . It is necessary to take into account the uncertainty of correction factor g only for the instrument I and when calibration is carried out in air [18]. The value of g factor for instrument II is well known and its uncertainty can be assumed negligible. Instrument I on the other hand does not take the g factor into account i.e. the value of g factor is taken as unity. The real value of the g factor for instrument I was determined experimentally. Its difference from unity was taken into account as a systematic uncertainty component if the instrument was calibrated in air.

Uncertainties of other input quantities. The standard uncertainties of the other input quantities S , H , p_n , $p_{\text{H}_2\text{O}_{100\%}}$, K_h^0 , P_{sme}^0 , R , A_1 , A_2 , A_3 , A_4 , A_5 , B_1 , B_2 , and B_3 do not have further sources.

7.2. Implicit Uncertainty Sources

Uncertainty of DO concentration in the calibration solution. The quantity $C_{\text{sat_cal_water}}$ as defined by eq 18 explicitly takes into account only the uncertainties of temperature and the coefficients of the model (uncertainty due to the imperfect accuracy of the model). There are two more sources of uncertainty that are not taken into account by the input quantities of eq 18:

- (1) Uncertainty of the reference methods of determining the DO concentration [25] used for compiling the tables of published values of saturated oxygen concentrations [4, 20].
- (2) Uncertainty arising from the imperfect fit of the mathematical model of oxygen saturation concentrations to the data [4, 20].

These uncertainty sources will be accounted for by means of introducing an additional quantity into the model: $\Delta C_{\text{sat_cal_water}}$.

Partial pressure of oxygen. The quantity W as defined by eq 19 allows to take into account the difference of atmospheric pressure from the standard atmospheric pressure during calibration and also the possible uncertainty due to imperfect saturation. However, there is an additional uncertainty in the oxygen content of the air used for saturation [4, 30, 31]. The main contribution of this is the unstable CO_2 content of the indoor air. The CO_2 content was monitored in the laboratory during calibration and the resulting uncertainty was estimated.

These uncertainty sources will be accounted for by means of an additional quantity in the model Δp_{CO_2} .

Uncertainty due to rounding of the digital reading. The uncertainty due to rounding of the digital reading is not explicitly taken into account. The reason is that the directly measured quantities indicating the oxygen concentration – the currents J_{meas} , J_{cal_water} and J_{cal_air} are not registered by the user. Instead the user reads directly the oxygen content C_{meas} from display. The uncertainty due to rounding of C_{meas} will be accounted for by means of two additional quantities in the model ΔC_{read_cal} and ΔC_{read_meas} .

Temperature instability of the calibration medium during calibration. The uncertainty of T_{cal} accounts for the uncertainty of temperature measurement during calibration. There is however an additional uncertainty source – uncertainty due to the mismatch between the temperature inside the sensor (which is actually measured by the instrument) and temperature in the calibration medium. There are two different media for calibrating the instruments: air and water. The instability and mismatch of temperature between the sensor and the calibration medium is taken into account by an additional quantity in the model, denoted as ΔT_{instab_water} and ΔT_{instab_air} in the calculation files for water and air, respectively, or generally as ΔT_{instab} . Different quantities are due to the vastly different magnitude of this uncertainty: in water the temperature equilibrium between the sensor body and calibration medium is significantly more stable and arrives faster than in air. The existence of these uncertainty sources makes it necessary to modify the eq 18. These uncertainty sources will be accounted for by means of an additional quantity in the equation as follows:

$$C_{sat_cal_water} = \exp \left(A_1 + \frac{A_2}{T_{cal} + \Delta T_{instab}} + \frac{A_3}{(T_{cal} + \Delta T_{instab})^2} + \frac{A_4}{(T_{cal} + \Delta T_{instab})^3} + \frac{A_5}{(T_{cal} + \Delta T_{instab})^4} \right) \quad (23)$$

Dependence of sensor current on the stirring speed. It is generally accepted that the sensor must be moved through the solution if accurate DO measurement results are desired [10, 16, 18]. If movement of the sensor in the medium is not ensured then decrease of oxygen concentration in the layer of test solution close to the membrane occurs. This way the effective diffusion layer thickness increases and the current decreases leading to underestimated results [10]. The optimum flow rate of solution past the membrane is about 30 cm sec⁻¹. It is appropriate to express the stirring speed here as linear velocity not as stirring angular velocity. This is because the sensor response is affected by the solution flow past the membrane, which remains undefined with angular velocity (depends on the distance of the sensor from the stirring axis). Dependence of the sensor current on the stirring speed of the solution is not explicitly taken into account by the eqs 14 and 16. We introduce an additional quantity ΔJ_{stir} (denoted as $\Delta J_{stir_calwater-meas}$ and $\Delta J_{stir_calair-meas}$) into our model to account for the

stirring effect. The definition of this quantity is described in eqs 24 to 27. No error is introduced if the stirring velocities during measurement and calibration are equal (see eq 24). In that case $u(\Delta J_{\text{stir}}) = 0$ A. In reality, however, there is mostly some mismatch between these two stirring speeds that introduces additional uncertainty into the measurement. The quantity ΔJ_{stir} is denoted differently for calibration in air and calibration in water: $\Delta J_{\text{stir_calwater-meas}}$ and $\Delta J_{\text{stir_calair-meas}}$. This is due to the somewhat different meaning of this quantity for the two different calibration procedures. $\Delta J_{\text{stir_calwater-meas}}$ takes into account the uncertainty introduced by the possible mismatch of the stirring speed in measured solution and in the calibration solution. $\Delta J_{\text{stir_calair-meas}}$ takes into account the possible mismatch between the stirring speed during measurement and the "effective stirring speed" during calibration in air, which after correcting with the g factor corresponds to the stirring speed 30 cm/s in water.

7.3. Quantifying the Uncertainty Components

Currents $J_{\text{meas_output}}$ and $J_{\text{cal_output}}$. As seen above the uncertainty of the quantities $J_{\text{meas_output}}$ and $J_{\text{cal_output}}$ is entirely due to repeatability uncertainty. All other current-related uncertainty sources are taken into account using additional quantities. The current repeatability in water is strongly dependent both on the current value and on the stirring speed. Stirring dependence of sensor output current repeatability is illustrated by figure 4. The repeatability uncertainty is proportional to the current value, thus relative standard uncertainties are given.

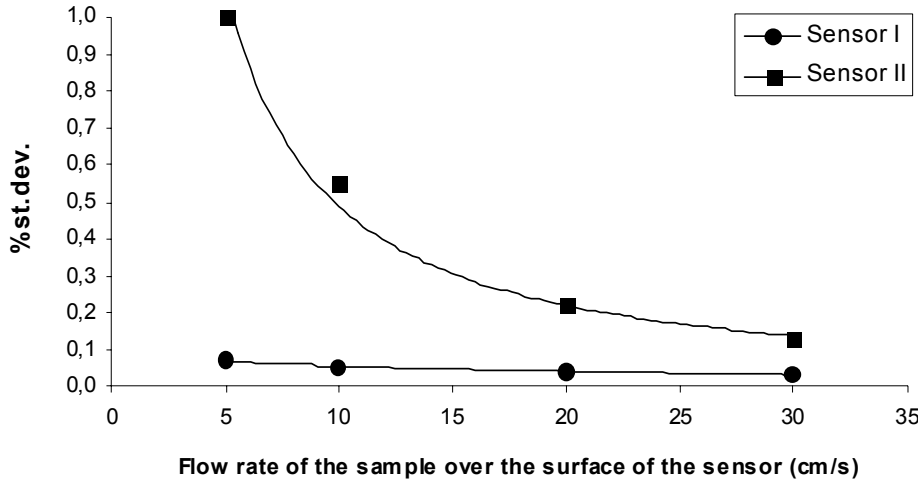


Figure 4. Stirring Dependence of Sensors Output Current Repeatability (at Water Temperature 20°C).

Repeatability of the sensor current in air has been found experimentally by measuring current in air saturated by water vapor at 20°C. The stirring speed effect is absent here. The repeatability values for the sensor I and II were 0.02% and 0.03 % of the current values.

ΔJ_{stir} . This is an auxiliary parameter introduced for taking into account the uncertainty due to the stirring effect (see section 7.2). The quantity ΔJ_{stir} is defined in such a way that its value is zero and its standard uncertainty is found using the following empirical equation:

$$u(\Delta J_{\text{stir}}) = \left| \frac{J_{\text{cal}}}{J_{\text{cal_max}}} - \frac{J_{\text{meas}}}{J_{\text{meas_max}}} \right| \cdot \frac{J_{\text{meas}}}{\sqrt{3}} \quad (24)$$

The maximum output current of the sensors in water $J_{\text{cal_max}}$ and $J_{\text{meas_max}}$ can be found using a factor Q :

$$J_{\text{cal_max}} = \frac{J_{\text{cal}}}{Q} \quad (25)$$

$$J_{\text{meas_max}} = \frac{J_{\text{meas}}}{Q} \quad (26)$$

The sensor current dependence on the stirring speed of the solution during calibration and measurement is described by the following empirical function:

$$Q = \frac{a \cdot v_{\text{stirring_speed}}}{b + v_{\text{stirring_speed}}} \quad (27)$$

where $v_{\text{stirring_speed}}$ [cm s^{-1}] is the stirring speed of the solution during calibration or measurement, a and b are constants. Their values were found experimentally and are 1.01 and 0.23 for sensor I and 1.03 and 0.90 for sensors II, respectively. The value of Q is thus in the range of around 0.85 to 1.

The dependence of the sensor current on stirring speed has been found experimentally by measuring current under saturation conditions at 20°C using different stirring speeds. The maximum current values $J_{\text{cal_max}}$ and $J_{\text{meas_max}}$ are those that correspond to sufficiently high (around 30 cm s^{-1}) stirring speed that leads to the virtual elimination of the stagnant solution layer (see above). Nevertheless, membrane porosity causes an additional diffusion layer of solution that is responsible for the value of the g factor in excess of 1. According to equation 24 the uncertainty is caused by mismatch of the stirring speed in the measured solution and in the calibration solution.

The stirring speed dependence of the sensor output current was measured in a cylindrical glass vessel with diameter 14.3 cm. The water in the cylinder was saturated with air and stirred at constant speed. The sensor was immersed into the solution and the reading was allowed to stabilize. The sensor was then

removed and maintaining the same stirring speed a glass triangle hanging on a thin cord (which did not hinder the free rotation of the triangle) was immersed into the solution. From the rotation frequency of the triangle the stirring speed – the speed of water moving past the sensor – was estimated.

The Zero Current J_0 . The zero current (which consists of the true zero current and the residual current) of the sensors is small, but cannot be considered negligible, especially at low DO concentrations. Our investigations reveal that the true zero current of both sensors is very low, but they both may have rather high residual current. Both instruments have built-in single-point calibration routine. This calibration assumes absence of zero current. Two-point calibration possibility, that would enable to take zero current into account during calibration is not provided by the manufacturers. Thus, in order to correspond to the situation with the real instruments, the parameter J_0 in all our calculations has zero value and the possible residual current is taken into account as the uncertainty of J_0 . The maximum value of J_0 for evaluating the $u(J_0)$ is determined in a solution that is devoid of oxygen as described in the experimental section [10, 15]. The zero current values for the sensors I and II were 0.52% and 0.97% of the corresponding current values (see figure 2). The relative standard uncertainty estimates (expressed as percentages) are obtained by dividing these values with $\sqrt{3}$.

Thickness of the diffusion layer $l_{\text{sme_cal}}$, $\Delta l_{\text{sme_drift}}$. The diffusion layer thickness during measurement is expressed as $l_{\text{sme_meas}} = l_{\text{sme_cal}} + \Delta l_{\text{sme_drift}}$. As described above, by definition the sensor currents during calibration do not have the explicit drift uncertainty component. The same applies to the diffusion layer thickness during calibration: $u(l_{\text{sme_cal}}) = 0$. The uncertainty due to the drift of the sensor parameters is in our approach taken into account as drift of the membrane thickness $\Delta l_{\text{sme_drift}}$, even though the drift is not fully due to the membrane thickness drift. The quantity $\Delta l_{\text{sme_drift}}$ is defined as having zero value, so that the expectation value of $l_{\text{sme_meas}}$ is equal to $l_{\text{sme_cal}}$. The uncertainty of $\Delta l_{\text{sme_drift}}$ takes into account the mismatch between the membrane thickness during measurement and calibration.

Based on our experience with DO measurement equipment we have estimated the drift uncertainties for the sensors under different conditions. The drift of two sensors was monitored during 2 months. The drift in sensor I was the highest with a new sensor. After one month of sensor usage the drift decreased. This finding confirms earlier similar reports [22]. With the sensor II the drift was also higher after cleaning the cathode and anode and replacing the membrane and the electrolyte. After being in use for some time the drift of this sensor also decreased. There are thus two different situations with respect to thickness of the diffusion layer:

1. With new sensor I drift during one day: $u(\Delta l_{\text{sme_drift}}) = 0.01 \text{ } \mu\text{m}$ (relative uncertainty 1.2% during one month) and sensor II 0.01 μm (relative uncertainty 2.3% during one month).

2. With old sensor I, drift during one day: $u(\Delta I_{\text{sme_drift}}) = 0.004 \mu\text{m}$ (relative uncertainty 0.5% during one month) and sensor II $0.004 \mu\text{m}$ (relative uncertainty 0.9% during one month).

Figure 5 illustrates the drift contributions.

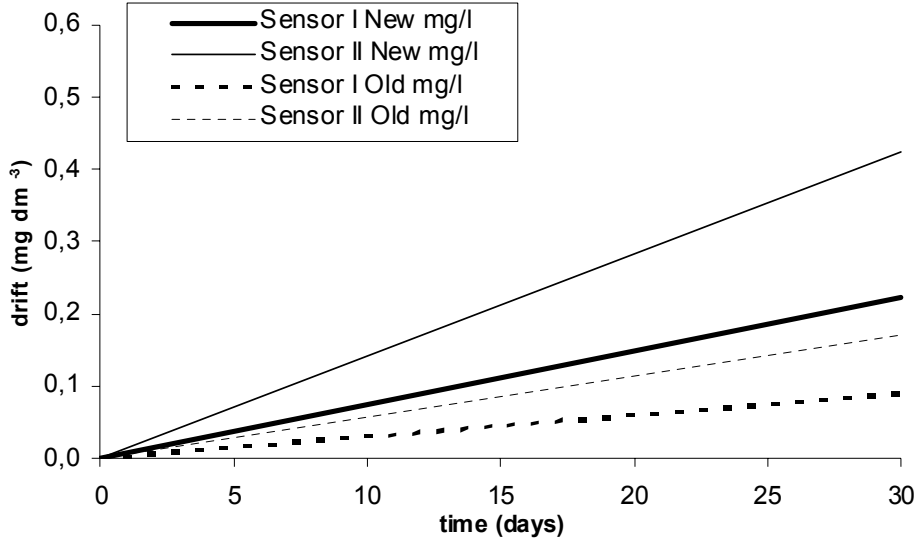


Figure 5. The Maximum Drift Uncertainty Contribution of the Sensors I and II Determined Separately for New and Old Sensors.

Activation energy of diffusion E_{sme} . We take the uncertainty caused by the mismatch between the E_{sme} of the actual membrane and the same parameter of an average membrane (for which the activation energy is preset into the meters by the manufacturers, see section 7.1) into account as $u(E_{\text{sme}})$. This uncertainty contribution has been measured as described in ref 23. From the experiments we can deduce that the standard uncertainty of the activation energy E_{sme} is: sensor I $u(E_{\text{sme}}) = 528 \text{ J mol}^{-1}$ and sensor II $u(E_{\text{sme}}) = 367 \text{ J mol}^{-1}$.

Drift of activation energy $E_{\text{sme_drift}}$. Changes in the activation energy E_{sme} of the sensors were monitored during 1 year (sensor I) or using several 6-months sessions (sensor II). The measurements were carried out at two temperatures: calibration at 20°C and measurement at 5°C . For the sensor I the average drift during one year of the DO concentration value measured at 5°C under saturation conditions was found to be equal to 0.20 mg dm^{-3} , which makes the uncertainty due to $\Delta E_{\text{sme_drift}}$ drift as $u(E_{\text{sme_drift}}) = 55 \text{ J (mol}\cdot\text{month)}^{-1}$. The drift of E_{sme} of the sensor II was negligible, so we take its uncertainty as $u(E_{\text{sme}}) = 0 \text{ J (mol}\cdot\text{month)}^{-1}$.

Temperature T_{meas} and T_{cal} . According to the documentation of the instruments, the uncertainties of all temperature measurements are ± 0.2 K ($k = 2$) [16] for the instrument I and ± 0.1 K ($k = 2$) for the instrument II. Our experiments have revealed that the uncertainty of temperature measurement of the instrument II can be almost two times higher than specified in the documentation. Therefore we use the same uncertainty estimate ± 0.2 K ($k = 2$) for both instruments and $u(T_{\text{cal}}) = 0.1$ K.

The calibration and measurement temperature values measured by the instruments are strongly correlated. The correlation leads to decreasing the effective uncertainty of T_{meas} with respect to the measurement. The decrease is the stronger the more similar are the temperatures. According to our experiments uncertainty of the measurement temperature can be described by the following equation:

$$u(T_{\text{meas}}) = |T_{\text{cal}} - T_{\text{meas}}| \cdot \frac{u(T_{\text{cal}})}{20} \quad (28)$$

where 20 [K] is an empirical constant. The equation is valid for both sensors.

Uncertainty of $\Delta C_{\text{sat_cal_water}}$. Numerous tables of saturated DO concentration values have been published [15, 20, 24, 30–38]. The differences between the data of different authors are generally in the order of 0.05 mg dm^{-3} [4]. It is assumed that these discrepancies come from the influence of two factors described for $\Delta C_{\text{sat_cal_water}}$ in the section 7.1. Based on the available data we estimate the uncertainty of $\Delta C_{\text{sat_cal_water}}$ as $\pm 0.05 \text{ mg dm}^{-3}$, that is $u(\Delta C_{\text{sat_cal_water}}) = 0.029 \text{ mg dm}^{-3}$. DO concentration in the calibration medium (when calibrating in water) was checked with Winkler titration (with uncertainty $\pm 0.05 \text{ mg dm}^{-3}$, $k = 2$).

Temperature instability of the calibration medium during calibration. The mismatch of temperature between the sensor and the calibration medium is taken into account by an additional quantity in the model, denoted as $\Delta T_{\text{instab_water}}$ and $\Delta T_{\text{instab_air}}$ in water and air respectively (see the explanations in section 7.2). We have obtained the following estimates for these uncertainty components: $u(\Delta T_{\text{instab_water}}) = 0.015$ K and in air $u(\Delta T_{\text{instab_air}}) = 0.1$ K.

Atmospheric pressure during calibration p_{cal} . The DO meter II has a built-in atmospheric pressure sensor and the standard uncertainty of pressure measurements according to our experiments is $u(p_{\text{cal}}) = 150$ Pa. In the case of the DO meter I measurement with external barometer with uncertainty $u(p_{\text{cal}}) = 100$ Pa was used. In those cases where measurement was deliberately carried out without atmospheric pressure correction we used the average pressure value 99700 Pa and $u(p_{\text{cal}}) = 1000$ Pa. this value and its uncertainty have been obtained during 2 years of monitoring atmospheric pressure in Estonia.

Partial pressure of water vapor $p_{\text{H}_2\text{O_cal}}$. The partial water vapor pressure in air saturated with water (at 100% relative humidity) both for aeration and direct calibration was measured with uncertainty $\pm 10\%$ ($k=2$) at our laboratory: $u(p_{\text{H}_2\text{O_cal}}) = 117 \text{ Pa}$ (at temperature 20°C).

Factor g . Our experiments have revealed that the real g factor for instrument I is 1.014. However, this instrument does not use a correction for this value, thus effectively assuming $g = 1$ and giving DO concentration values that are systematically low by 1.4%. This systematic effect is included in the uncertainty budget as an uncertainty component. The standard uncertainty of g factor (actually: the mismatch between the real and the used g factors) is found by dividing difference 0.014 by $\sqrt{3}$ giving $u(g) = 0.008$.

Uncertainties of the constants A_1 , A_2 , A_3 , A_4 , A_5 , B_1 , B_2 , and B_3 . The uncertainties of these constants reflect the imperfections of the mathematical models presented by eq 18 and 20, respectively and have been taken into account by the additional term $\Delta C_{\text{sat_cal_water}}$. Therefore these constants are handled in the calculation as quantities without uncertainty.

8. THE FINAL MATHEMATICAL MODEL

The existence of implicit uncertainty sources makes it necessary to improve the mathematical model in such a way that it would allow to take into account all identified uncertainty sources. The necessary additional quantities and their roles in the model have been described in section 7.2. The final mathematical model with all the uncertainty sources is:

$$C_{\text{meas}} = \left(\frac{(J_{\text{meas_output}} + \Delta J_{\text{stir}} - J_0) \cdot (I_{\text{sme_cal}} + \Delta I_{\text{sme_drift}})}{(J_{\text{cal_output}} - J_0) \cdot I_{\text{sme_cal}}} \right) \cdot \left(\exp \left(\frac{E_{\text{sme}} + \Delta E_{\text{sme_drift}} + H}{R} \cdot \left(\frac{1}{T_{\text{cal}}} - \frac{1}{T_{\text{meas}}} \right) \right) \right) \cdot \left(\frac{p_{\text{cal}} - p_{\text{H}_2\text{O_cal}} + \Delta p_{\text{CO}_2}}{p_{\text{n}} - p_{\text{H}_2\text{O_100\%}}} \right) \cdot (C_{\text{sat_cal_water}} + \Delta C_{\text{sat_cal_water}} + \Delta C_{\text{read_cal}}) \cdot g + \Delta C_{\text{read_meas}} \quad (29)$$

where $C_{\text{sat_cal_water}}$ is defined by eq 23. The model permits to take into account the uncertainties of all the included parameters thereby covering all the uncertainty sources discussed above. The uncertainty due to the imperfection of the model itself is accounted for by three input quantities. The uncertainty of E_{sme} covers the uncertainty due to deviation of the actual temperature dependence of permeability from that included in the model. The uncertainty of $\Delta C_{\text{sat_cal_water}}$ takes into account the imperfection of the equation describing temperature dependence of saturation concentration of DO in water. The uncertainty of $p_{\text{H}_2\text{O_cal}}$ takes into account the imperfection of the equation of temperature dependence of water vapor partial pressure in air. In article I there were 11 influence factors taken into consideration. In this final model 18 influence factors are taken into account [II]. In addition to those taken into account already in the original model the following factors are now accounted for: stirring effect, two different drifts for new and old sensor, drift of the membrane activation energy, uncertainty contribution of the g factor if calibration has been made in air, temperature instability of the calibration medium, uncertainty due to rounding of the digital reading. Additionally the correlation effect between the parameters T_{meas} and T_{cal} has been taken into account.

9. RESULTS AND DISCUSSION

Below we present application of the above described model to two DO measurement instruments under real-life measurement conditions by investigating 5 different measurement cases. The results and the uncertainty budgets of the 5 cases are presented in tables 1 and 2.

Table 1. Measurement Conditions and Uncertainty Budgets of the Results obtained by Instruments I and II Corresponding to the Cases 1 – 5 Using Calibration in Water.

Inputs	Case 1		Case 2		Case 3		Case 4		Case 5	
calibration	water		water		water		water		water	
environment										
Instrument	I	II	I	II	I	II	I	II	I	II
Measurement conditions										
C_{meas} (mg dm ⁻³)	9.00	9.00	9.00	9.00	1.00	1.00	5.00	5.00	5.00	5.00
t_{meas} (°C) ^a	20	20	20	20	20	20	5	5	5	5
stirring speed_meas (cm s ⁻¹)	30	30	15	15	30	30	10	10	15	15
t_{cal} (°C) ^a	20	20	20	20	20	20	20	20	20	20
$u(p_{\text{cal}})$ (Pa)	100	150	100	150	100	150	100	150	100	150
stirring speed_cal (cm s ⁻¹)	30	30	15	15	30	30	20	20	20	20
$\Delta\text{day_new}_{\Delta\text{cal-meas}}$ (day)	0	0	0	0	0	0	5	5	0	0
$\Delta\text{day_old}_{\Delta\text{cal-meas}}$ (day)	0	0	0	0	0	0	0	0	15	15
Δmonth (month)	0	0	0	0	0	0	0.5	0.5	6	6
Input Parameters (x_i) ^b	Uncertainty contributions (indexes) of the input parameters x_i									
t_{cal}	22%	0%	22%	0%	1%	0%	2%	0%	2%	0%
ΔT_{instab}	0%	1%	0%	0%	0%	0%	0%	0%	0%	0%
ΔJ_0	0%	0%	0%	0%	40%	99%	38%	18%	37%	45%
$\Delta J_{\text{cal_output}}$	0%	12%	0%	31%	0%	0%	0%	1%	0%	1%
p_{cal}	3%	15%	3%	8%	0%	0%	0%	0%	0%	1%
$\Delta C_{\text{sat_cal_water}}$	19%	49%	19%	25%	1%	0%	2%	1%	2%	2%
Δp_{CO_2}	0%	1%	0%	0%	0%	0%	0%	0%	0%	0%
$\Delta p_{\text{H}_2\text{O_cal}}$	4%	9%	4%	5%	0%	0%	0%	0%	0%	0%
$\Delta C_{\text{read_cal}}$	26%	0%	25%	0%	1%	0%	2%	0%	2%	0%
t_{meas}	0%	0%	0%	0%	0%	0%	5%	0%	5%	1%
$\Delta J_{\text{meas_output}}$	0%	12%	0%	31%	0%	0%	0%	3%	0%	3%
$\Delta \bar{C}_{\text{read_meas}}$	26%	1%	26%	0%	58%	0%	8%	0%	7%	0%
$\Delta I_{\text{sme_drift}}$	0%	0%	0%	0%	0%	0%	1%	2%	1%	0%
$\Delta E_{\text{sme_drift}}$	0%	0%	0%	0%	0%	0%	0%	0%	12%	0%
ΔJ_{stir}	0%	0%	0%	0%	0%	0%	10%	67%	1%	20%
$E_{\text{sme_membrane}}$	0%	0%	0%	0%	0%	0%	32%	8%	30%	20%
Expanded uncertainties ($k = 2$) of C_{meas}										
$U(C_{\text{meas}})$	0.11	0.07	0.11	0.10	0.08	0.09	0.21	0.29	0.21	0.18
$U(C_{\text{meas}})$, relative	1.3%	0.8%	1.3%	1.1%	7.6%	8.9%	4.2%	5.7%	4.2%	3.6%

^a t_{meas} (°C) = T_{meas} (K) – 273.15 and t_{cal} (°C) = T_{cal} (K) – 273.15

^b Please see the section 7 Uncertainty Sources for definitions.

Table 2. Measurement Conditions and Uncertainty Budgets of the Results obtained by Instruments I and II Corresponding to the Cases 1 – 5 Using Calibration in Air.

Inputs calibration environment Instrument	Case 1 air		Case 2 air		Case 3 air		Case 4 air		Case 5 air	
	I	II	I	II	I	II	I	II	I	II
Measurement conditions										
C_{meas} (mg dm ⁻³)	9.00	9.00	9.00	9.00	1.00	1.00	5.00	5.00	5.00	5.00
t_{meas} (°C) ^a	20	20	20	20	20	20	5	5	5	5
stirring speed_meas (cm s ⁻¹)	30	30	15	15	30	30	10	10	15	15
t_{cal} (°C) ^a	20	20	20	20	20	20	20	20	20	20
$u(p_{\text{cal}})$ (Pa)	100	150	100	150	100	150	100	150	100	150
stirring speed_cal (cm s ⁻¹)	30	30	30	30	30	30	30	30	30	30
g (–) ^c	(eq)	(eq)	(eq)	(eq)	(eq)	(eq)	(eq)	(eq)	(eq)	(eq)
$\Delta\text{day_new}_{\Delta\text{cal-meas}}$ (day)	–	1.017	–	1.017	–	1.017	–	1.017	–	1.017
$\Delta\text{day_old}_{\Delta\text{cal-meas}}$ (day)	0	0	0	0	0	0	5	5	0	0
Δmonth (month)	0	0	0	0	0	0	0	0	15	15
Δmonth (month)	0	0	0	0	0	0	0.5	0.5	6	6
Input Parameters (x_i)^b	Uncertainty contributions (indexes) of the input parameters x_i									
t_{cal}	8%	0%	7%	0%	1%	0%	2%	0%	2%	0%
ΔT_{instab}	4%	22%	3%	1%	0%	0%	1%	0%	1%	1%
ΔJ_0	0%	0%	0%	0%	38%	99%	30%	12%	31%	28%
$\Delta J_{\text{cal output}}$	0%	1%	0%	0%	0%	0%	0%	0%	0%	0%
p_{cal}	1%	13%	1%	1%	0%	0%	0%	0%	0%	0%
$\Delta C_{\text{sat cal water}}$	7%	43%	6%	3%	1%	0%	1%	1%	1%	1%
Δp_{CO_2}	0%	1%	0%	0%	0%	0%	0%	0%	0%	0%
$\Delta p_{\text{H}_2\text{O cal}}$	1%	8%	1%	0%	0%	0%	0%	0%	0%	0%
$\Delta C_{\text{read cal}}$	9%	0%	8%	0%	1%	0%	2%	0%	2%	0%
g	60%	0%	50%	0%	4%	0%	12%	0%	12%	0%
t_{meas}	0%	0%	0%	0%	0%	0%	4%	0%	4%	1%
$\Delta J_{\text{meas output}}$	0%	11%	0%	3%	0%	0%	0%	2%	0%	2%
$\Delta C_{\text{read meas}}$	9%	1%	8%	0%	56%	0%	6%	0%	6%	0%
$\Delta I_{\text{sme drift}}$	0%	0%	0%	0%	0%	0%	1%	1%	1%	4%
$\Delta E_{\text{sme drift}}$	0%	0%	0%	0%	0%	0%	0%	0%	10%	0%
ΔJ_{stir}	0%	0%	17%	91%	0%	0%	15%	79%	4%	50%
$E_{\text{sme membrane}}$	0%	0%	0%	0%	0%	0%	25%	5%	25%	12%
Expanded uncertainties ($k = 2$) of C_{meas}										
$U(C_{\text{meas}})$	0.19	0.08	0.21	0.31	0.08	0.09	0.23	0.36	0.23	0.23
$U(C_{\text{meas}})$, relative	2.1%	0.8%	2.3%	3.4%	7.7%	9.0%	4.7%	7.2%	4.6%	4.6%

^a t_{meas} (°C) = T_{meas} (K) – 273.15 and t_{cal} (°C) = T_{cal} (K) – 273.15

^b Please see the section 7 Uncertainty Sources for definitions.

^c The instrument I does not take the g factor into account. The instrument II g factor is 1.017. The g factor has been found under optimum stirring conditions (30 cm s⁻¹, see the section Implicit Uncertainty Sources).

The cases have been selected to mimic as closely as possible real-life measurement conditions and to provide possibility to compare the performance of the two different instrument designs. Presented below are the main findings of the uncertainty analysis. The cases 1–3 model laboratory conditions: calibration was carried out immediately before measurement, measurement temperature was equal to calibration temperature, the membranes of both sensors were new. In the cases 4–5 measurement conditions mimic those of routine environmental measurements: calibration is carried out in laboratory several days (or even few weeks) before measurement, calibration and measurement temperatures are different.

Case 1: Measurement and calibration temperatures are the identical. Calibration has been carried out under saturation conditions, either in water (table 1) or in air (table 2) immediately before measurement. The stirring speed is the same during measurement and calibration and is quite high: 30 cm s^{-1} . DO concentration is relatively high (9 mg dm^{-3}).

Under these conditions uncertainty is lower with the instrument II than with the instrument I, especially when calibration is carried out in air. When examining the contributions of different uncertainty sources one finds that different uncertainty sources dominate for different instruments. In the case of the instrument I calibrated in water the dominating uncertainty contribution is the uncertainty due to rounding of the digital reading (52%). It is followed by the uncertainty contribution from calibration temperature measurement (22%) and the uncertainty of DO concentration of saturated solution (19%). If calibration is carried out in air then the single dominating uncertainty contribution is introduced by the absence of the g value in the instrument. This instrument does not take the difference between calibration in water and calibration in air into account thus making an uncorrected systematic error. In our approach this error is included in the uncertainty budget as an uncertainty component and its contribution is large: 60%.

The main uncertainty contribution in the case of the instrument II under these conditions comes from the limited accuracy of the saturation concentration of DO. This contribution amounts to 49% or 43% for calibration in water and air respectively. If we would neglect all other uncertainty contributions then the relative expanded uncertainty would decrease from 0.8% to 0.6% for calibration both in water and in air. Thus the source of a major part of the uncertainty in this instance is extraneous to the instrument. Following this prominent uncertainty source comes the temperature uncertainty in the case of calibration in air or repeatability uncertainty in the case of calibration in water.

The case 1 corresponds to the ideal working conditions for the instruments and the smallest uncertainties that can be obtained with them. Detailed description of the calculations and the full uncertainty budget can be found in appendixes 2 and 3.

The instrument I does not have a built-in atmospheric pressure sensor. In the above case it is assumed that the user takes the atmospheric pressure into account when calibrating the instrument. If this is not so, then the uncertainty of the instrument I increases heavily: from 1.3% to 2.4% and the uncertainty due to atmospheric pressure forms 70% of the overall uncertainty.

It is very appropriate to stress here the importance of saturation with water vapor of the air that is in turn used for saturating the calibration water. If this is not done then the oxygen content of the air is higher than in the published tables by around 2% (calculated by equation 19 at temperature 20°C) and if this systematic effect is included into the uncertainty budget then the uncertainty increases significantly: from 1.3% to 2.4%. The dominating component is then the mismatch between oxygen content in the used dry air and in the air saturated with water, accounting for 74% of the overall uncertainty.

Case 2. The conditions are the same as in Case 1, except that the stirring speed is lower: 15 cm s⁻¹.

One can see that differently from Case 1 the uncertainties of the results obtained by the two instruments are more similar when the stirring speed is lower. The structure of the uncertainty budgets, however, continues to be different. Significant differences are evident also between calibration in water and in air.

In the case of instrument I calibrated in water the uncertainty budget and the uncertainty itself are practically identical to that of Case 1. When calibrating this instrument in air then the most important uncertainty contribution is the missing g factor (50%). This uncertainty source is followed by the uncertainty due to the mismatch of the actual stirring speed during measurement and the equivalent stirring speed of calibration in air (17%). The high stirring speed suppressed the influence of this uncertainty component in Case 1.

In the case of the instrument II the structure of the uncertainty budget continues to be different from the instrument I. In the case of calibration in water 62% of the uncertainty is caused by current repeatability contributions. The lower current stability is not unexpected: the cathode area of the sensor is around 1000 times smaller in sensor II than in sensor I and the instability of the additional diffusion layer between the membrane and the bulk solution has more influence on the output signal of the sensor at low stirring speeds. This uncertainty contribution is followed by the uncertainty of saturated DO concentration (25%). The picture is yet completely different when the calibration of the instrument II is carried out in air: 91% of the uncertainty is caused by the possible stirring speed mismatch between calibration and measurement! Also the overall uncertainty is more than three times higher than when calibrating the instrument in water. Again in Case 1 the high stirring speed largely masked the difference between calibration in air and water by

compressing the stagnant diffusion layer and decreasing the uncertainty associated with it. At lower stirring speed this situation does not hold any more.

Based on this result a word of caution is necessary with respect to the recommendations of manufacturers to calibrate DO measurement instruments of this type in air. The user must be aware that although calibration in air is very convenient, high stirring speed during measurement is extremely important when calibration has been performed in air.

Case 3: The same conditions as in Case 1, except that measurement is carried out in solution where the DO concentration is low: 1 mg dm^{-3} instead of 9 mg dm^{-3} .

The uncertainties delivered by the two instruments are similar, while the structures of the uncertainty budgets are totally different. In this case the differences between calibration in water and in air are insignificant due to the high stirring speed.

The uncertainty budget of the instrument I is dominated by the uncertainty of rounding the digital reading, which makes up 58 and 56% of the uncertainty when calibrating in water and in air, respectively. This is followed by the uncertainty due to the zero current of the sensor (40 and 38%). All other uncertainty sources are insignificant. The uncertainty budget of the instrument II is heavily dominated by the uncertainty of the zero current: 99%. In part this dominance is caused by the two-decimal-digits readout of the instrument (this makes the digital readout uncertainty contribution ten times lower than in the case of instrument I). However, even if the readout had just one decimal digit the uncertainty contribution due to zero current would still account for 70% of the uncertainty and the contribution due to rounding would be only 11%. The intrinsically higher share of the zero current uncertainty comes from the higher residual current in the case of the sensor II. If the readout of the DO meter I had one more digit then the uncertainty would fall from 7.6–7.7% to around 5.0% thereby being around 1.5 times lower than that of the instrument II.

Case 4. Calibration was carried out in laboratory at 20°C (stirring speed 20 cm s^{-1}) five days before measurement. The measurement is performed under out-door conditions in water at 5°C . The estimated stirring speed during measurement is 10 cm s^{-1} (this is a proper estimate of the speed in the case of a slow river or moving the sensor up and down during measurement). The DO concentration is 5 mg dm^{-3} . The sensors are new (ca 2 weeks old).

The uncertainties of the instruments differ and the uncertainty budgets are again totally different.

In the case of the instrument I the largest uncertainty contributions are due to the possible mismatch between the actual membrane parameters and those that

are used by the instrument in performing temperature corrections and uncertainty due to the zero current of the sensor. These contributions are of nearly equal importance and jointly contribute 70% and 55% of the overall uncertainty when calibrating in water and air, respectively. It is possible to reduce the influence of the zero current of the sensor by allowing the reading to stabilize more than 2 minutes (the residual current will still decrease). These two contributions are followed by the stirring speed mismatch between calibration and measurement (10% and 15% in the case of calibration in water and in air, respectively).

In the case of the instrument II the stirring speed mismatch is heavily dominating the uncertainty budget contributing 67–79% of the overall uncertainty. This heavy dominance together with high uncertainty is due to the thinner and more permeable FEP membrane of the sensor II compared to the PP membrane of the sensor I. This indicates that the thicker is the membrane and the lower is its permeability the less is the sensor sensitive to stirring speed and changes of the electrolyte layer thickness and thus the more stable and rugged is the sensor [5]. This uncertainty source alone is responsible for the higher uncertainty of the instrument II. The downside of the thicker and less permeable membrane of the sensor I is the longer time needed for stabilization of the reading.

Case 5: In this case the conditions are similar to Case 4, except that old (6 months) sensors were used and the stirring speed during measurement was 15 cm s^{-1} and calibration was carried out 15 days before the measurement.

For the instrument I similarly to Case 4 uncertainty due to the zero current has a large share. However, now it is just one of the dominating uncertainty contributions together with the contributions from the drift of the membrane properties and the mismatch between the actual E_{me} and the value stored in the meter. Emerging of the drift of the membrane properties as an important uncertainty source is directly connected to the age of the sensor membrane 6 months. The overall uncertainty is also slightly higher. All other components can be considered negligibly small and the uncertainty budgets for calibration in water and in air are very similar.

In the case of the instrument II the uncertainty has dropped around 1.5 times from Case 4. This has happened because the stirring speed is now higher. As can be expected the stirring effect, although still prominent, is not the largest uncertainty contribution anymore. Instead it is the zero current contributing 45% and 28% of the overall uncertainty, although its absolute contribution is the same as in Case 4. Differently from the sensor I the membrane properties drift has negligible influence with sensor II. This is due to the membrane material (FEP) that has more stable properties. All in all one can say that the membrane material of the sensor II is better, both from the point of view of stability and characterization uncertainty.

Figure 6 visualizes the trends in overall uncertainties when calibrating the instruments in water and in air.

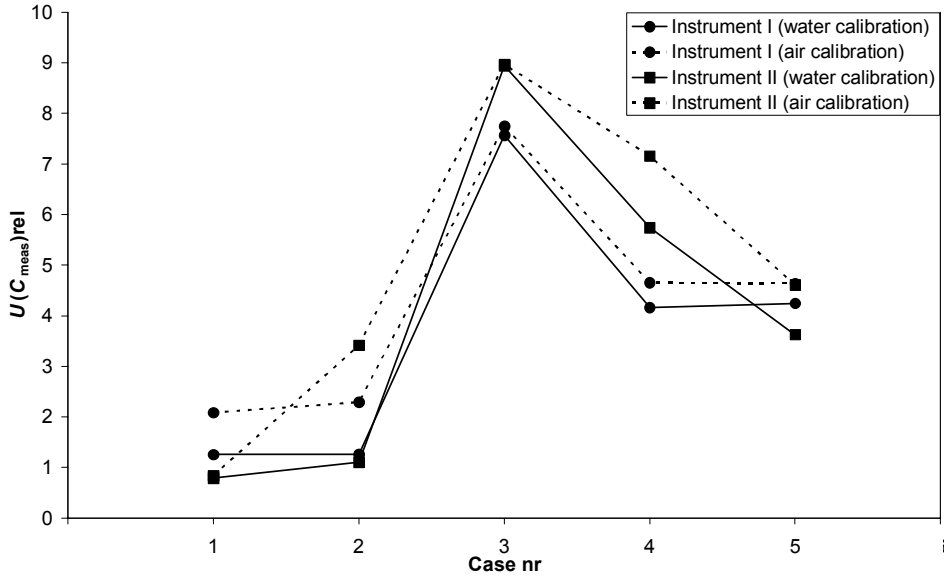


Figure 6. The Relative Uncertainties of DO Concentrations Measured with Instruments I and II Calibrated in Air and in Water. The points have been connected for better readability.

Implications for DO sensor design. Without doubt the following features are highly desirable in DO sensor design: *temperature sensor* permitting automatic temperature correction, *pressure sensor* permitting taking the atmospheric pressure into account during calibration.

Membrane material. From tables 1 and 2 it follows that as soon as measurement temperature is different from calibration temperature – a usual situation in the case of environmental measurements – the uncertainty of the activation energy of diffusion of oxygen through membrane E_{sme} becomes a major uncertainty source. The membrane material quality, i.e. batch-to-batch reproducibility and stability against ageing and fouling, is thus of utmost importance. In order to provide the user possibility to compensate for the drift of E_{sme} it would be very helpful to incorporate the possibility of calibrating at two different temperatures into the instrument as this would allow to adjust E_{sme} on a regular basis.

Membrane thickness and permeability are a more complex issue. The thinner is the membrane (or the higher the permeability) the shorter is the reading stabilization time. At the same time the current is less stable and the drift of the sensor is higher (the distance between membrane and cathode is less stable) and

the danger of damaging the membrane is higher. If air calibration possibility is desired then incorporation of the g -factor into the instrument is critical, otherwise its absence becomes a major (under some conditions dominating) uncertainty source. Thicker membrane (or lower membrane permeability) gives the sensor ruggedness, higher stability, lower drift and lower sensitivity towards stirring speed. At the same time such sensor cannot be used for studying process kinetics (unless the process is really slow) and it requires careful waiting for reading stabilization.

The areas of cathode, anode and membrane. Large cathode and membrane area gives stable current. Large cathode and anode area gives longer sensor lifetime (cathode: lower load of fouling agents like H_2S per area unit of cathode; anode: larger area of anode takes longer to oxidize). At the same time sensor with larger cathode and membrane areas consumes more oxygen from the measured solution. Thus if measurement is carried out in a closed system where DO content is finite it may be impossible to get a correct value. Membrane area should not be larger than cathode area, otherwise a side-diffusion process results that decreases the stability of the sensor current. Instead it is good if cathode area is somewhat larger than membrane area.

The larger is the cathode area relative to the volume of the plastic parts of the sensor and the electrolyte the lower is the zero current of the sensor. Tables 1 and 2 indicate that reducing the zero current would be one of the most efficient ways to reduce uncertainty in measurement of DO at low levels.

10. DISSOLVED OXYGEN *IN SITU* INTERLABORATORY COMPARISON

Dissolved oxygen is an unstable analyte. Thus preparation of reference solutions that are stable for extended period of time is complicated or outright impossible. This complicates the standardization of the measurement and organization of interlaboratory comparisons [III]. It is difficult to make the intercomparisons with sending samples to the participating laboratories as is usually done in the case of interlaboratory comparisons in other chemical measurements. Instead the comparison measurements have to be carried out at the same time on the same site (*in situ*) and all the participants have to travel to that site. Organization of the *in situ* interlaboratory comparison measurements of dissolved oxygen concentration at University of Tartu started in 2004 and have taken place three times until today: on March 2, 2004, February 3, 2005 [III] and March 7, 2006 at Department of Chemistry, University of Tartu.

10.1. Description of the *in situ* ILC Apparatus and Measurement Conditions

Water thermostat U-10 (manufactured in the former Eastern Germany) with temperature stability of $\pm 0.01^{\circ}\text{C}$ (in 2004 and 2005) or water thermostat CC2-K12 (manufactured in Germany) with temperature stability of $\pm 0.03^{\circ}\text{C}$ (in 2006) was used for thermostating. DO concentrations and temperatures were changed in a 4 dm^3 vessel that contained 3.9 dm^3 (l) of distilled water (2004, 2005) or in a vessel containing 12 dm^3 of distilled water (2006). The vessel was seated in the thermostat. The air, which was used for saturating the distilled water in the thermostat, was in turn saturated by water vapor according to the conditions of the standard [15].

The solution was stirred with constant speed. The DO sensors of the participants were arranged concentrically in the bath and were immersed approximately to the same depth. This setup permitted to achieve the best possible uniformity of the measurement conditions between the participants.

Temperature was measured by calibrated digital thermometer Chub-E4 (model nr 1529, serial nr A44623, manufacturer Hart Scientific) with two Pt100 sensors (ser. no. 0818 and 0855). The uncertainties of all temperature measurements were $\pm 0.05^{\circ}\text{C}$. Air pressure was measured by aneroid barometer Bamm-1, nr 8858 (manufactured in the former Soviet Union in 1974). Evaluated uncertainty is 200 Pa ($k=2$).

10.2. Reference Values and their Uncertainties

The reference values were found using eq 18 according to the standard [15]. Uncertainties of the references values where estimated according to ISO GUM method [11]. The mathematic model is described in section 4. Additionally, we have taken into account possible dissolved oxygen concentration inhomogeneity in solution (between the sensors of participants). The mathematical model for calculating uncertainty of reference value based on equations 19, 20 and 23. The reference values and uncertainties are given in table 3. The correctness of reference values was determined by Winkler iodometric titration methods as the reference method (according to ISO 5813:1983) [25].

Table 3. Reference Values and Uncertainties of Dissolved Oxygen *in situ* Inter-laboratory Comparison.

ILC of 2004		ILC of 2005		ILC of 2006	
Ref (mg dm ⁻³)	U, k=2	Ref (mg dm ⁻³)	U, k=2	Ref (mg dm ⁻³)	U, k=2
6.84	0.10	8.36	0.15	8.18	0.15
8.17	0.10	9.22	0.15	9.01	0.15
9.97	0.10	10.20	0.15	10.01	0.15
12.63	0.10	12.91	0.15	12.71	0.15

10.3. Results of the Instrument I Participating to the *in situ* ILC

The instrument I participated in all three intercomparison rounds. The results and uncertainties of instrument I participating to the *in situ* ILC are given in the table 4. The uncertainties have been estimated according to the above-described procedure. E_n numbers [39] were used to assess the agreement between Instrument I values and the reference values. The E_n numbers are found as follows:

$$E_n = \frac{C_{\text{lab}} - C_{\text{ref}}}{\sqrt{U_{\text{lab}}^2 + U_{\text{ref}}^2}};$$

where C_{lab} is the Instrument I DO result, C_{ref} is the reference value of DO concentration, U_{lab} is the expanded uncertainty of the Instrument I result and U_{ref} is the expanded uncertainty of the reference value.

Criteria for laboratory performance based on the E_n numbers:

- a) $|E_n| \leq 1$: satisfactory (the result and reference value are accordant);
- b) $|E_n| > 1$: unsatisfactory (the result and reference value are not accordant).

The E_n number values are presented in table 4.

Table 4. Instrument I Values and Uncertainties participating to the Dissolved Oxygen *in situ* Interlaboratory Comparison.

ILC of 2004			ILC of 2005			ILC of 2006		
Instru- ment I (mg dm ⁻³)	U, k=2	Instru- ment I <i>E_n</i> number	Instru- ment I (mg dm ⁻³)	U, k=2	Instru- ment I <i>E_n</i> number	Instru- ment I (mg dm ⁻³)	U, k=2	Instru- ment I <i>E_n</i> number
7.0	0.3	1.0	8.2	0.3	0.5	8.1	0.3	0.3
8.3	0.2	0.6	9.2	0.3	0.1	8.9	0.3	0.4
10.1	0.2	0.4	10.3	0.3	0.3	9.9	0.3	0.3
12.5	0.2	0.4	13.2	0.4	0.7	12.4	0.5	0.6

In all cases the E_n numbers indicate agreement between the ILC reference values and the results of the instrument I thus supporting the validity of the uncertainty estimates obtained for the instrument I.

SUMMARY

A result of this work uncertainty estimation procedure based on mathematical model of dissolved oxygen electrochemical (galvanic type) measurement was developed. The procedure involves identification and quantification of individual uncertainty sources according to the ISO GUM approach. This procedure was applied to the two different galvanic type instruments. The uncertainty budgets of the results are very different depending on the instrument as well as on measurement conditions. Variations in the relative expanded uncertainty between $U = 0.8\%$ to $U = 9\%$ ($k = 2$) were observed for the same instrument under different conditions. At DO concentrations lower than below 4 mg dm^{-3} (depending on other conditions) the background current of the sensor becomes the dominating uncertainty source. At DO concentrations above that range, a variety of influence factors become relevant depending on the specific conditions, for example stirring speed and membrane properties. The high importance of the cathode and membrane area, membrane material and membrane thickness on the uncertainty was demonstrated. Based on these results a set of recommendations for DO sensor design was formulated. Evidence that the obtained uncertainty estimates are realistic was obtained from participating to *in situ* ILCs. All the E_n numbers calculated using the developed procedure were below value 1.

SUMMARY IN ESTONIAN

Käesolevas uurimuses töötati välja elektrokeemilise amperomeetrilise lahustunud hapniku analüsaatori matemaatiline mudel ja mõõtmistulemuse määramatuse hindamise protseduur. Protseuur baseerub ISO GUM meetodil, mis sisaldab määramatuse allikate identifitseerimist ja kvantiseerimist. Määramatuse hindamise protseduuri rakendati kahele galvaanilist tüüpi analüsaatorile. Leiti, et mõõtmistulemuse määramatus ja üksikkomponentide osakaal kogu määramatusest sõltub tugevalt nii analüsaatorist kui ka mõõtmiste tingimustest: suhteline laiendmääramatus erinevates mõõtmistingimustes varieerub vahemikus $U = 0.8\%$ kuni $U = 9\%$ ($k = 2$). Kui lahustunud hapniku sisaldus on madalam kui 4 mg dm^{-3} on nullvoolu määramatuse komponent domineeriv. Kõrgematel kontsentratsioonidel ja madalal segamiskiirusel on olulisimaks komponendiks madalast segamiskiirusest tulenev määramatus. Kalibreerimistemperatuurist oluliselt erinevatel mõõtmistemperatuuridel osutuvad oluliseks membraani parameetrite (hapniku difusiooni aktivatsioonienergia ning selle triiv) määramatuse komponendid. Analüsaatori mõõtmistulemuste usaldusväärsuse seisukohast on olulised järgmised konstruktsioonilised parameetrid: katoodi pindala, membraani materjal ja membraani paksus. Lähtuvalt saadud tulemustest formuleeriti analüsaatori optimaalse konstruktsiooni põhiseisukohad. Määramatuse hinnangute realistlikkust kinnitavad läbiviidud *in situ* võrdlusmõõtmiste tulemused: hälbed referentsväärtustest jäid alati määramatuse piiridesse.

REFERENCES

1. Chang S C, Stetter J R, and Cha C S 1993 *Talanta* **40** 461
2. Hobbs B S, Tantrum A D S and Chan-Henry R 1991 *Liquid Electrolyte Fuel Cells, Techniques and Mechanisms in Gas Sensing*, Adam Hilger, Bristol
3. Mashirin A, Koorits A and Tenno T 1986 *Acta et Comment. Univ. Tartuensis* **743** 77
4. Hellat K, Mashirin A, Nei L and Tenno T 1986 *Acta et Comment. Univ. Tartuensis* **757** 184
5. Dawson F H and Henville P 1985 *J. Phys. E: Sci. Instrum.* **18** 526
6. Sable Systems International, Oxygen electrodes -how they work and what to do when they don't. <http://www.sablesys.com>
7. Nösel H 1973 *Messtechnik* **1** 15
8. YSI incorporated Model 95 Handheld Dissolved Oxygen and Temperature System Operations Manual 1998 <http://www.ysi.com>
9. Instruction Manual 2001 General Cybernetics Corporation, O2xBOX Dissolved Oxygen Analyser <http://www.generalcybernetics.com>
10. Hitchman M L 1978 *Measurement of Dissolved Oxygen* (NewYork: Wiley) ch 5 71–123
11. BIPM, IEC, IFCC, ISO, IUPAC, IUPAP, OIML 1993 *Guide to the Expression of Uncertainty in Measurement* (Geneva: International Organization for Standardization)
12. Ellison S L R, Rösslein M and Williams A (eds) 2000 *Quantifying Uncertainty in Analytical Measurement* 2nd edn. EURACHEM/CITAC
13. Papadakis I and Taylor P D P 2001 *Accred. Qual. Assur.* **6** 466
14. Wilcock R J, Stevenson C D and Roberts C A 1981 *Water Res.* **15** 321
15. ISO 5814 Water quality – Determination of dissolved oxygen – Electrochemical probe method 1990
16. Instruction Manual for Model MJ2000 2000 *Elke Sensor LLC* Estonia
17. Operating Manual 2004 *Wissenschaftlich-Technische Werkstätten GmbH* Germany, Dissolved Oxygen Pocket Meter Oxi330i/Oxi340i and Operating Manual 2002 Dissolved Oxygen Sensor CelloX 325
18. Principles of Measuring Technique 2001 Edition 5 CD *Wissenschaftlich-Technische Werkstätten GmbH* Germany
19. Tenno T 1986 *Acta et Comment. Univ. Tartuensis* **757** 166
20. Mortimer C H 1981 *Mitt Int Ver Limnol* **22** 1
21. Albantov A F and Levin A L 1994 *Biosensors and Bioelectronics* **9** 515
22. Nei L and Compton R G 1996 *Sensors and Actuators B* **30** 83
23. Jäetma T 1992 M.Sc. Thesis Tallinn Technical University
24. Benson B B and Krause D 1980 *Limnol. Oceanogr.* **25** 662
25. ISO 5813 Water quality – Determination of dissolved oxygen – Iodometric method 1983
26. Jeroschewski P and Linden D 1997 *Fresenius J. Anal. Chem.* **358** 677
27. Owens B and Millard R 1985 *Journal of Physical Oceanography* **15** 621
28. Tenno T, Mashirin A, Raudsepp I, Past V 1978 *Acta et Comment. Univ. Tartuensis* **441** 138

29. Tenno T, Tamm L, Bergmann K and Past V 1976 *Acta et Comment. Univ. Tartuensis* **378** 108
30. Landine R C 1971 *Water and Sewage Works* **118** 242
31. Truesdale G A, Downing A L and Lowden G F 1955 *J. Appl. Chem.* **5** 53
32. Carpenter J H 1966 *Limnol. Oceanogr.* **11(2)** 264
33. Murray C N and Riley J P 1969 *Deep-Sea Res.* **16** 311
34. Montgomery A C and Thom N S 1964 *J. Appl. Chem.* **14** 280
35. Elmore H L and Hayes T W 1960 *J. San. Eng. Div.* **86** 41
36. Green E J and Carritt D E 1967 *J. Mar. Res.* **25** 140
37. Weiss R F 1970 *Deep-Sea Res.* **17** 721
38. American Public Health Association 1975 Standard methods for the examination of water and waste water 14th ed
39. ISO/IEC Guide 43–1 Proficiency Testing by Interlaboratory Comparisons. Part 1: Development and Operation of Proficiency Testing Schemes 1997

ACKNOWLEDGEMENTS

I would like to thank my supervisor Professor Ivo Leito for his self-sacrificing help and constantly positive way of thinking. I am deeply indebted to Professor Toomas Tenno, Mr Aleksei Maširin and Mr Viktor Vabson for helpful discussions.

Also I would like to thank Dr Viljar Pihl and Dr Ivari Kaljurand for good advice and valuable comments.

Mrs Ester Uibopuu, Mr Priit Nigu, Mrs Anne Paaver, Dr Viljar Pihl and Mr Teet Jäetma: thank you for supplying technical equipment.

My special thanks to my colleagues: Dr Lilli Sooväli, Dr Eve Koort, Ms Agnes Kütt, Ms Kristina Virro, Mrs Marju Rosenthal, Dr Olev Saks, Dr Viljar Pihl, Dr Ivari Kaljurand and Dr Koit Herodes for warm and supporting atmosphere.

I am very thankful to my family for support. Ms Sille Siniavski thank you for the help with translation.

I would like to thank my friend Dr Lauri Toom who made it easier for me access the world of scientific articles.

This work was supported by the grant 5475 from the Estonian Science Foundation and by the basis financing funds (project 06902) of the University of Tartu and by a scholarship from the World Federation of Scientists.

APPENDIX 1

Appendix 1

Calculation K_{0_h} [(Pa(O₂)-dm³) mg⁻¹ J (the oxygen partition pre-exponential coefficient) and H [J mol⁻¹] (the oxygen dissolution enthalpy in water) values

R	8,314	J/(K*mol)	
%O ₂	0,2095	O ₂ content in air %	Oxygen concentration of air-saturated distilled water [mg dm ⁻³]
p _n	101325	Pa	
A ₁	-139,3441	-	
A ₂	1,58E+05	-	
A ₃	-6,64E+07	-	
A ₄	1,24E+10	-	
A ₅	-8,62E+11	-	
B ₁	11,8571	-	
B ₂	-3840,7	-	
B ₃	-216961	-	

$$C_{\text{sat_cal_wa}} = \exp \left(A_1 + \frac{A_2}{T_{\text{sat}}} + \frac{A_3}{(T_{\text{sat}})^2} + \frac{A_4}{(T_{\text{sat}})^3} + \frac{A_5}{(T_{\text{sat}})^4} \right)$$

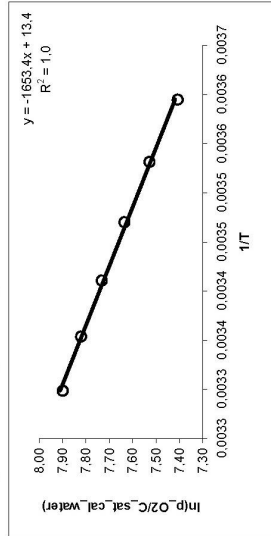
Oxygen partial pressure in water saturated air [Pa]:

$$p_{O_2} = (p_n - p_{H_2O,100\%}) \cdot 0.2095$$

Water vapor pressure at 100% relative humidity [Pa]

$$p_{H_2O,100\%} = p_n \cdot \exp \left(\frac{B_1}{T_{\text{sat}}} + \frac{B_2}{T_{\text{sat}}^2} + \frac{B_3}{(T_{\text{sat}})^3} \right)$$

t (C)	T (K)	1/T	p _{O2} (Pa)	p _{H2O,100%} (Pa)	W	C _{sat_cal_water} (mg/dm ³)	ln(p _{O2} /C _{sat_cal_water})
5,0	278,2	0,00359518	21045	872	1	12,77	7,41
10,0	283,15	0,0035317	20970	1228	1	11,29	7,53
15,0	288,15	0,00347041	20870	1705	1	10,08	7,64
20,0	293,15	0,00341122	20738	2338	1	9,09	7,73
25,0	298,15	0,00335402	20564	3168	1	8,26	7,82
30,0	303,15	0,0032987	20339	4243	1	7,56	7,90



The partial pressure of oxygen, the partition coefficient of oxygen between water and the gas phase – the Henry's constant – and the concentration of DO are linked by the Henry's law

$$p_{O_2} = K_h \cdot C_{\text{sat_cal_wa}}^{\text{ter}}$$

K_h depends on temperature according to the following equation

$$K_h = K_h^0 \cdot e^{\frac{H}{RT}}$$

The equations can be united to give:

$$\ln \left(\frac{p_{O_2}}{C_{\text{sat_cal_water}}} \right) = \frac{H}{R} \cdot \frac{1}{T} + \ln K_h^0$$

slope

intercept

Kh_H_Pame_Esme_calculations

```
function (LINEST):
    slope=-1653,4    13,3634=intercept
    s(slope)=43,5636    0,1501=s(intercept)
    x20,9972    0,0108=regression standard deviation
```

Calculated values:
H -13747 J/mol
K_h_0 636288 (PaO2*dm3)/mg

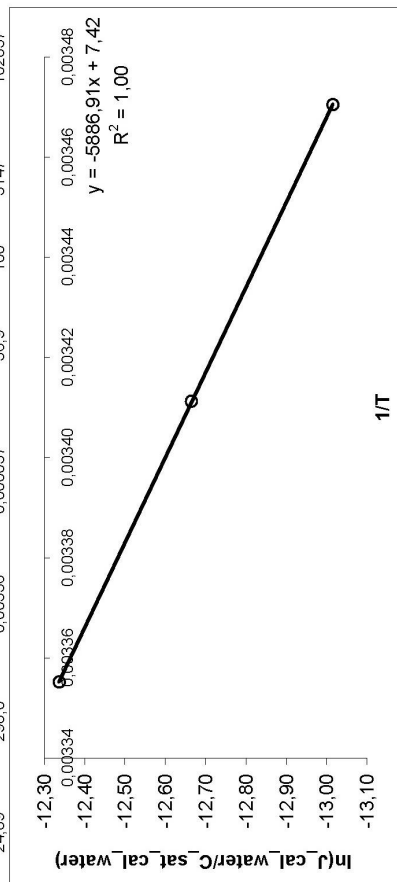
Kh_H_Peme_Esme_calculations

Calculation P_sme_0 and E_sme values for Sensor I

Measurements were performed in air-saturated water (at 100% relative humidity) at several constant temperatures

Membrane: polypropylene (PP) membrane with thickness 0,0025 cm

Constants for calculation of saturation values in water													
p, n	A ₁	101325	Pa										-139.3441
	A ₂	4											1.58E+05
	A ₃	96485	C/mol										-6.64E+07
	A ₄	5.265	cm2										1.24E+10
	A ₅	0.0025	cm										-8.62E+11
S	L _{sme} *	0.0025											
	%O ₂	0.2095	O2 content in air %										
	R	8.314	J/(K*mol)										
Constants for calculation water saturated partial pressure in air													
	B ₁												11.8571
	B ₂												-3840.7
	B ₃												-216961
Constants for calculation water saturated partial pressure in air													
t cal (C)	T cal (K)	1/T	J cal water (A)	J cal water (B)	RH*	p H2O cal (Pa)	p cal (Pa)	W	C_sat cal water (mg/dm3)	ln(J cal water)	C_sat cal water		
14.99	288.1	0.00347	0.000023	22.8	100	1704	102805	1.01	10.24	-13.02			
19.99	293.1	0.00341	0.000029	29.2	100	2337	102805	1.01	9.23	-12.66			
24.89	298.0	0.00336	0.000037	36.9	100	3147	102857	1.02	8.41	-12.34			



Kh H Psme Esme calculations

```
function (LINEST):
    slope=-5886.9 / 7.4159=intercept
    s(slope)=23.5627 / 0.0804=s(intercept)
    r=1.0000 / 0.0019=regression standard deviation
```

Results:

H ^o E _{sme}	-48947	J/mol
K _h 0 ^o P _{sme} 0	2,05E-06	(mol ³ dm ³)/(cm ³ sek*mg)

Data for calculations from the previous sheet

H	-13747	J/mol
Kh_0	636288	(PaO2*dm3)/mg

Calculated values:

E _{sme}	-35199	J/mol
P _{sme} 0	3,21E-12	mol/(cm ³ sek*Pa(O2))

Unit analysis:

$$J_{cal_water} = n \cdot F \cdot S \cdot \frac{1}{l_{sme_cal}} \cdot P_h^0 \cdot K_h^0 \cdot e^{\frac{E_{sme}+H}{RT_{sat}}} \cdot C_{sat_cal_wa_ter} \cdot W$$
$$[J_{cal_water}] = \frac{C}{cm^2} \cdot \frac{mol}{cm \cdot s} \cdot \frac{Pa \cdot dm^3}{mg} \cdot \frac{mg}{dm^3} \cdot \frac{C}{s} = A$$

* Membrane thickness (*l_m*) is used as the approximation of the *l_{sme}* value. This approximation is justified, because: (1) The value of *l_m*/*P_m* is by far the largest contributor to the *l_{sme}*/*P_{sme}* (2) The same approximation is done by calibration and by measurement thus the effect cancels out

APPENDIX 2

Input values for uncertainty analysis				
	Value	Unit	Comments and U, k=2	st. uncertainty
Input values for calibration (calibration in air-saturated water:)				
t_{cal}	20	C	0,2	0,10
ΔT_{instab_water}	0	C	0,03	0,02
J_0	0	A	0,60%	8,5E-08
$\Delta J_{cal_output_water}$	0	A	0,06%	8,8E-09
p_{cal}	99700	Pa	200	100
$\Delta C_{sat_cal_water}$	0	mg/l	0,05	0,025
Δp_{CO_2}	0	Pa	0,07%	35
$p_{H_2O_cal}$	100	%RH	10%	5,0%
ΔC_{read_cal}	0	mg/l	0,06	0,03
$stirringspeed_cal$	30	cm/s		
addition input values for air calibration (Calibration in air saturated with water vapor:)				
ΔT_{instab_air}	0	C	0,2	0,10
g	1	-	1,62%	0,008
$\Delta J_{cal_output_air}$	0	A	0,04%	5,6E-09
Input values for measurement				
t_{meas}	20	C	0,00	0,00
ΔJ_{meas_output}	0	A	0,06%	8,9E-09
C_{meas}	9,00	mg/l		
ΔC_{read_meas}	0	mg/l	0,06	0,03
$stirringspeed_meas$	30	cm/s		
drift section for new and old membrane and electrolyte				
$\Delta l_{sme_dpd_new}$	0	cm/day	0,0000020	0,000001
$\Delta day_new_{\Delta cal-meas}$	0	day		
$\Delta l_{sme_drift_new}$	0	cm		0,00E+00
$l_{sme_dpd_old}$	0	cm/day	0,0000008	0,0000004
$\Delta day_old_{\Delta cal-meas}$	0	day		
$\Delta l_{sme_drift_old}$	0	cm		0,00E+00
$\Delta month$	0	month		
E_{sme_dpm}	0	J/(mol*month)	110	55
ΔE_{sme_drift}	0	J/mol		0
Calculated values for calibration (calibration in air-saturated water:)				
J_{cal_water}	2,82E-05	A		
$J_{cal_output_water}$	2,8E-05	A		
T_{cal}	293,2	K		
P_{sme_cal}	1,7E-18	mol/(cm*sek*Pa(O ₂))		
K_{h_cal}	2260	Pa(O ₂)*dm ³ /mg		
$C_{sat_cal_water}$	9,09	mg/l		
$p_{H_2O_cal}$	2338	Pa	234	117
$p_{H_2O_100\%}$	2338	Pa		
W	0,98			
$stirringspeed_ \%max_value_cal_water$	1,00			
Calculated values for air calibration (Calibration in air saturated with water vapor:)				
J_{cal_air}	2,8E-05	A		
$J_{cal_output_air}$	2,8E-05	A		
$C_{sat_cal_air}$	9,09	mg/l		
$stirring_ \%max_value_cal_air$	1,00			

Instrument_I_uncertainty

Page 1

Input sheet

Appendix 2

Calculated values for measurement				
J_{meas}	2,8E-05	A		
$J_{\text{meas_output}}$	2,8E-05	A		
T_{meas}	293,2	K		
$P_{\text{sme_meas}}$	1,7E-18	mol/(cm*sek*Pa(O ₂))		
$K_{\text{h_meas}}$	2260	Pa(O ₂)*dm ³ /mg		
stirring_%max_value_meas	1,00	-		
$\Delta J_{\text{stir_calwater-meas}}$	0	A	0,0E+00	0,0E+00
$\Delta J_{\text{stir_calair-meas}}$	0	A	2,2E-08	1,1E-08
Probe characteristics				
Type		Value	Unit	
Cathode				Galvanic Cr/Ni
S	5,265		cm ²	
Anode				Pb
Membrane				polypropylene (PP)
Electrolyte solution				27% KOH
$l_{\text{sme_cal}}$	0,0025		cm	
P_{sme0}	3,21E-12		mol/(cm*sek*Pa(O ₂))	
E_{sme}	-35199		J/mol	3% -528
Constants				
A_1	-139,3441			function constant
A_2	1,58E+05			function constant
A_3	-6,64E+07			function constant
A_4	1,24E+10			function constant
A_5	-8,62E+11			function constant
B_1	11,8571			function constant
B_2	-3840,7			function constant
B_3	-216961			function constant
T_0	273,15		K	
K_{h0}	636288		Pa(O ₂)*dm ³ /mg	
H	-13747		J/mol	
n	4		-	
F	96485		C/mol	
R	8,31447		J/(K*mol)	
p_n	101325		Pa	

Estimation of Uncertainty in Electrochemical Amperometric Measurement of Dissolved Oxygen Concentration
Department of Chemistry, University of Tartu, Jakobi 2, 51014 Tartu, Estonia (2007)

Input values and uncertaintys for calculation

	Value	Unit	u	u/10	results
lcal	20	C	0.100	0.010	22%
DTrnsfab_water	0	C	0.015	0.002	0%
J0	0	A	0.000	0.000	0%
Dlcal_output_water	0	A	0.000	0.000	0%
pcal	99700	Pa	100.000	10.000	3%
DCal_Lcal_water	0	mg/l	0.025	0.003	19%
DpCO2	0	Pa	34.895	3.490	0%
pH2O_cal	2338	Pa	117	11.690	4%
DRead_cal	0	mg/l	0.029	0.003	26%
tmeas	20	C	0.000	0.000	0%
Dlmeas_output	0	A	0.000	0.000	0%
DRead_meas	0	mg/l	0.029	0.003	26%
Dsme_drift_new	0	cm	0.000	0.000	0%
Dsme_drift_old	0	cm	0.000	0.000	0%
DEsme_drift	0	J/mol	0.000	0.000	0%
DUsitr_calwater-meas	0	A	0.000	0.000	0%
Esme	-35199	J/mol	-528	-52.799	100%
J_cal_water	2.82E-05	A			
J_meas	2.84E-05	A			
Psme_cal	1.72E-18	mol/(cm²*sek*Pa(O2))			
Psme_meas	1.72E-18	mol/(cm²*sek*Pa(O2))			
Kl_cal	2260	Pa(O2)*dm3/mg			
Kl_meas	2260	Pa(O2)*dm3/mg			
Lsme_meas	2.50E-03	cm			
W	0.99				
Csal_cal_water	9.09	mg/l			
Cmeas	9.00	mg/l			
U, k=1	0.06	U, k=1			
U, k=2	0.11	U, k=2			
%	1.3	%			

Appendix 2

total	D\Tinstab_water	J0	D\cal_output_water	pcal	DCsat_cal_water	DpCO2	pH2O_cal	DCread_cal
20,01	20	20	20	20	20	20	20	20
0	0,00	0	0	0	0	0	0	0
0	0	8,48E-09	0	0	0	0	0	0
0	0	0	8,82E-10	0	0	0	0	0
99700	99700	99700	99700	99710,000	99700	99700	99700	99700
0	0	0	0	0	0,003	0	0	0
0	0	0	0	0	0	0	3	0
2338	2338	2338	2338	2338	2338	2338	2350	2338
0	0	0	0	0	0	0	0	0,003
20	20	20	20	20	20	20	20	20
0	0	0	0	0	0	0	0	0
0	0	0	0	0	0	0	0	0
0	0	0	0	0	0	0	0	0
0	0	0	0	0	0	0	0	0
0	0	0	0	0	0	0	0	0
0	0	0	0	0	0	0	0	0
-35199	-35199	-35199	-35199	-35199	-35199	-35199	-35199	-35199
2,82E-05	2,82E-05	2,82E-05	2,82E-05	2,82E-05	2,82E-05	2,82E-05	2,82E-05	2,82E-05
2,84E-05	2,84E-05	2,84E-05	2,84E-05	2,84E-05	2,84E-05	2,84E-05	2,84E-05	2,84E-05
1,7189E-18	1,7189E-18	1,7189E-18	1,7189E-18	1,7189E-18	1,7189E-18	1,7189E-18	1,7189E-18	1,7189E-18
1,7189E-18	1,7189E-18	1,7189E-18	1,7189E-18	1,7189E-18	1,7189E-18	1,7189E-18	1,7189E-18	1,7189E-18
2260	2260	2260	2260	2260	2260	2260	2260	2260
2260	2260	2260	2260	2260	2260	2260	2260	2260
2,50E-03	2,50E-03	2,50E-03	2,50E-03	2,50E-03	2,50E-03	2,50E-03	2,50E-03	2,50E-03
0,98	0,98	0,98	0,98	0,98	0,98	0,98	0,98	0,98
9,09	9,09	9,09	9,09	9,09	9,10	9,09	9,10	9,10
9,00	9,00	9,00	9,00	9,00	9,00	9,00	9,00	9,00
2,6E-03	-2,7E-04	-1,7E-05	-2,8E-04	9,2E-04	2,5E-03	3,2E-04	-1,1E-03	2,9E-03
7,0E-06	7,2E-08	2,9E-10	7,9E-08	8,5E-07	6,1E-06	1,0E-07	1,2E-06	8,2E-06
total	D\Tinstab_water	J0	D\cal_output_water	pcal	DCsat_cal_water	DpCO2	pH2O_cal	DCread_cal
21,9%	0,2%	0,0%	0,2%	2,7%	19,1%	0,3%	3,7%	25,5%

Instrument_I_uncertainty

Page 4

calculation_water_calibration

Appendix 2

Imeas	DImeas_output	DCread_meas	Dlsme_drift_new	Dlsme_drift_old	DEsme_drift	Dlsir_calwater-meas	Esme
	20	20	20	20	20	20	20
	0	0	0	0	0	0	0
	0	0	0	0	0	0	0
	0	0	0	0	0	0	0
99700	99700	99700	99700	99700	99700	99700	99700
0	0	0	0	0	0	0	0
0	0	0	0	0	0	0	0
2338	2338	2338	2338	2338	2338	2338	2338
0	0	0	0	0	0	0	0
20,000	20	20	20	20	20	20	20
0	0,000	0	0	0	0	0	0
0	0	0,002887	0	0	0	0	0
0	0	0	0,0E+00	0,0000	0	0	0
0	0	0	0	0,0000	0,0000	0	0
0	0	0	0	0	0	0	0
0	0	0	0	0	0	0,000	0
-35199	-35199	-35199	-35199	-35199	-35199	-35199	-35252
2,82E-05	2,82E-05	2,82E-05	2,82E-05	2,82E-05	2,82E-05	2,82E-05	2,82E-05
2,84E-05	2,84E-05	2,84E-05	2,84E-05	2,84E-05	2,84E-05	2,84E-05	2,84E-05
1,7189E-18	1,7189E-18	1,7189E-18	1,7189E-18	1,7189E-18	1,7189E-18	1,68206E-18	1,68206E-18
1,7189E-18	1,7189E-18	1,7189E-18	1,7189E-18	1,7189E-18	1,7189E-18	1,7189E-18	1,68206E-18
2260	2260	2260	2260	2260	2260	2260	2260
2260	2260	2260	2260	2260	2260	2260	2260
2,50E-03	2,50E-03	2,50E-03	2,50E-03	2,50E-03	2,50E-03	2,50E-03	2,50E-03
0,98	0,98	0,98	0,98	0,98	0,98	0,98	0,98
9,09	9,09	9,09	9,09	9,09	9,09	9,09	9,09
9,00	9,00	9,00	9,00	9,00	9,00	9,00	9,00
0,0E+00	2,8E-04	2,9E-03	0,0E+00	0,0E+00	0,0E+00	0,0E+00	0,0E+00 diff
0,0E+00	7,9E-08	8,3E-06	0,0E+00	0,0E+00	0,0E+00	0,0E+00	0,0E+00 diff*2
							3,2E-05 sum(diff*2)
Imeas	DImeas_output	DCread_meas	Dlsme_drift_new	Dlsme_drift_old	DEsme_drift	Dlsir_calwater-meas	Esme
0,0%	0,2%	26,1%	0,0%	0,0%	0,0%	0,0%	0,0%
							100,0% sum(index)

Instrument_I_uncertainty

Page 5

calculation_water_calibration

Input values and uncertaintys for calculation

	Value	Unit	u	u/10	results
ical	20	C	0.100	0.010	%
DTinstab_air	0	C	0.100	0.010	8%
J0	0	A	0.000	0.000	4%
D0cal_output_air	0	A	0.000	0.000	0%
p0cal	99700	Pa	100,000	10,000	0%
DCsat_cal_water	0	mg/l	0.025	0.003	1%
DpCO2	0	Pa	34,895	3,490	7%
pH2O_cal	2338	Pa	117	11,690	0%
D0read_cal	0	mg/l	0.029	0.003	1%
g	1	-	0.008	0.001	9%
timeas	20	C	0.000	0.000	60%
Dumeas_output	0	A	0.000	0.000	0%
D0read_meas	0	mg/l	0.029	0.003	0%
Disme_drift_new	0	cm	0.000	0.000	9%
Disme_drift_old	0	cm	0.000	0.000	0%
DESme_drift	0	J/mol	0.000	0.000	0%
D0stir_calair-meas	0	A	0.000	0.000	0%
Esme	-35199	J/mol	-528	-52,799	0%
J_cal_air	2,82E-05	A			100%
J_meas	2,84E-05	A			
Psme_cal	1,72E-18	mol/(cm²*sek*Pa(O2))			
Psme_meas	1,72E-18	mol/(cm²*sek*Pa(O2))			
Kh_cal	2260	Pa(O2)*dm3/mg			
Kh_meas	2260	Pa(O2)*dm3/mg			
L_sme_meas	2,50E-03	cm			
W	0,96				
Csat_cal_air	9,09	mg/l			
Cmeas	9,00	mg/l			
u, k=1	0,09				
U, k=2	0,19				
U, k=2	2,1	%			

60

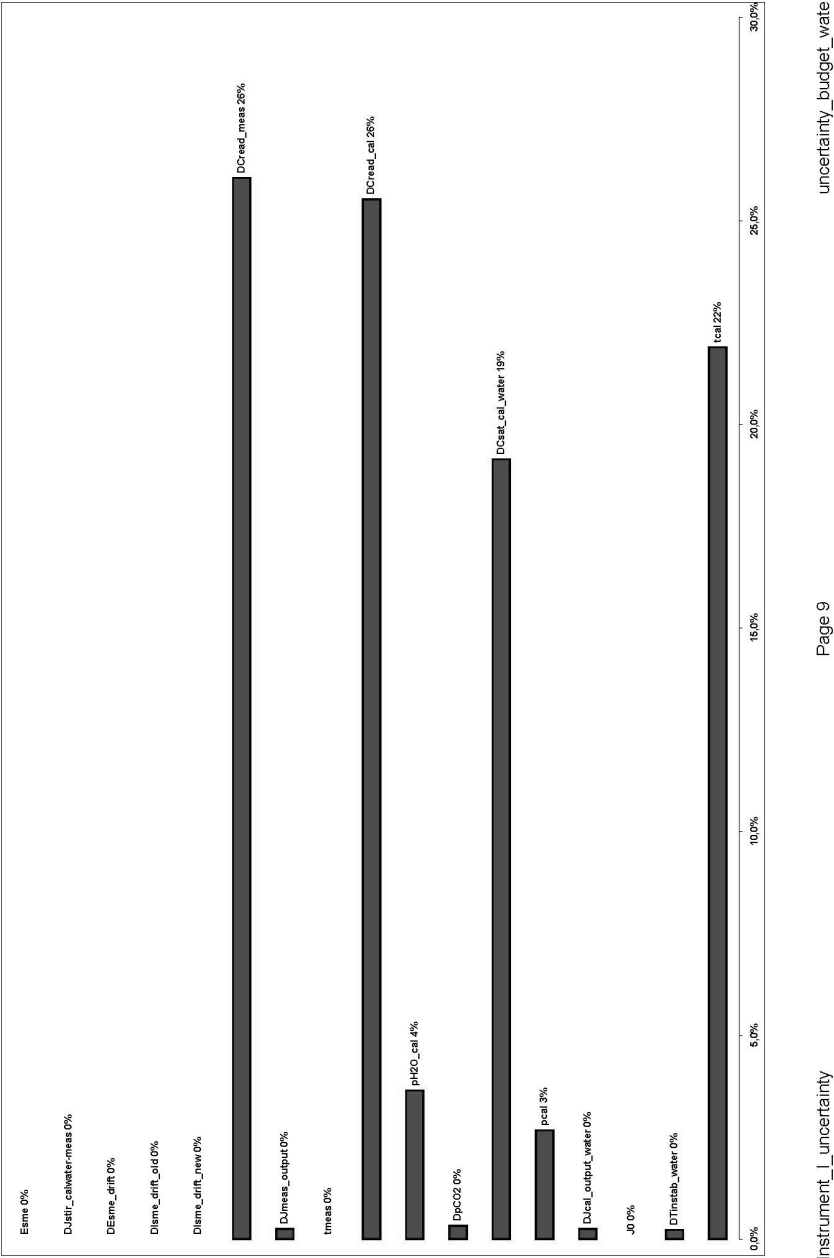
Instrument_1_uncertainty

Imeas	Dmeas_output	DCread_meas	Dsme_drift_new	Dsme_drift_old	DEsme_drift	Dustir_calair-meas	Esme
	20	20	20	20	20	20	20
	0	0	0	0	0	0	0
	0	0	0	0	0	0	0
	0	0	0	0	0	0	0
	99700	99700	99700	99700	99700	99700	99700
	0	0	0	0	0	0	0
	0	0	0	0	0	0	0
2337,998529	2337,998529	2337,998529	2337,998529	2337,998529	2337,998529	2337,998529	2337,998529
	0	0	0	0	0	0	0
	1	1	1	1	1	1	1
	20,000	20	20	20	20	20	20
	0	0,000	0	0	0	0	0
	0	0	0,002887	0	0	0	0
	0	0	0	0,0E+00	0	0	0
	0	0	0	0,000	0	0	0
	0	0	0	0	0,000	0	0
	0	0	0	0	0	0,000	0
-35199,21229	-35199,21229	-35199	-35199,21229	-35199,21229	-35199,21229	-35199,21229	-35252,011
2,82E-05	2,82E-05	2,82E-05	2,82E-05	2,82E-05	2,82E-05	2,82E-05	2,82E-05
2,84E-05	2,84E-05	2,84E-05	2,84E-05	2,84E-05	2,84E-05	2,84E-05	2,84E-05
1,7189E-18	1,7189E-18	1,7189E-18	1,7189E-18	1,7189E-18	1,7189E-18	1,7189E-18	1,6820E-18
1,7189E-18	1,7189E-18	1,7189E-18	1,7189E-18	1,7189E-18	1,7189E-18	1,7189E-18	1,6820E-18
2260	2260	2260	2260	2260	2260	2260	2260
2260	2260	2260	2260	2260	2260	2260	2260
2,50E-03	2,50E-03	2,50E-03	2,50E-03	2,50E-03	2,50E-03	2,50E-03	2,50E-03
0,98	0,98	0,98	0,98	0,98	0,98	0,98	0,98
9,09	9,09	9,09	9,09	9,09	9,09	9,09	9,09
9,00	9,00	9,00	9,00	9,00	9,00	9,00	9,00
0,0E+00	2,8E-04	2,9E-03	0,0E+00	0,0E+00	0,0E+00	3,4E-04	0,0E+00 diff
0,0E+00	7,9E-08	8,3E-06	0,0E+00	0,0E+00	0,0E+00	1,2E-07	0,0E+00 diff^2
							0,00009 sum(diff^2)
0,0%	Dmeas_output	DCread_meas	Dsme_drift_new	Dsme_drift_old	DEsme_drift	Dustir_calair-meas	Esme
	0,1%	9,5%	0,0%	0,0%	0,0%	0,1%	0,0%
							100,0% sum(index)

Instrument_I_uncertainty

Page 8

calculation_air_calibration



Appendix 2



Instrument_I_uncertainty

Page 10

uncertainty_budget_air

APPENDIX 3

Input values for uncertainty analysis				
	Value	Unit	Comments and U, k=2	st. uncertainty
Input values for calibration (calibration in air-saturated water:)				
t_{cal}	20	C	0,2	0,10
ΔT_{instab_water}	0	C	0,03	0,02
J_0	0	A	1,12%	1,3E-09
$\Delta J_{cal_output_water}$	0	A	0,27%	3,1E-10
p_{cal}	99700	Pa	300	150
$\Delta C_{sat_cal_water}$	0	mg/l	0,05	0,025
Δp_{CO_2}	0	Pa	0,07%	35
$p_{H_2O_cal}$	100	%RH	10%	5,0%
ΔC_{read_cal}	0	mg/l	-	
stirringspeed_cal	30	cm/s		
addition input values for air calibration (Calibration in air saturated with water vapor:)				
ΔT_{instab_air}	0	C	0,2	0,10
g	1,017	-		
$\Delta J_{cal_output_air}$	0	A	0,06%	6,9E-11
Input values for measurement				
t_{meas}	20	C	0,00	0,00
ΔJ_{meas_output}	0	A	0,27%	3,1E-10
C_{meas}	9,00	mg/l		
ΔC_{read_meas}	0	mg/l	0,01	0,00
stirringspeed_meas	30	cm/s		
drift section for new and old membrane and electrolyte				
$\Delta I_{sme_dpd_new}$	0	cm/day	0,0000020	0,000001
$\Delta day_new_{\Delta cal-meas}$	0	day		
$\Delta I_{sme_drift_new}$	0	cm		0,00E+00
$I_{sme_dpd_old}$	0	cm/day	0,0000008	0,0000004
$\Delta day_old_{\Delta cal-meas}$	0	day		
$\Delta I_{sme_drift_old}$	0	cm		0,00E+00
$\Delta month$	0	month		
E_{sme_dpm}	0	J/(mol*month)	0	0
ΔE_{sme_drift}	0	J/mol		0
Calculated values for calibration (calibration in air-saturated water:)				
J_{cal_water}	2,27E-07	A		
$J_{cal_output_water}$	2,3E-07	A		
T_{cal}	293,2	K		
p_{sme_cal}	6,7E-18	mol/(cm*sek*Pa(O ₂))		
K_{h_cal}	2260	Pa(O ₂)*dm ³ /mg		
$C_{sat_cal_water}$	9,09	mg/l		
$p_{H_2O_cal}$	2338	Pa	234	117
$p_{H_2O_100\%}$	2338	Pa		
W	0,98			
stirringspeed_%max_value_cal_water	1,00			
Calculated values for air calibration (Calibration in air saturated with water vapor:)				
J_{cal_air}	2,3E-07	A		
$J_{cal_output_air}$	2,3E-07	A		
$C_{sat_cal_air}$	9,25	mg/l		
stirling_%max_value_cal_air	1,00			

Instrument_II_uncertainty

Page 1

Input sheet

Calculated values for measurement				
J_{meas}	2,3E-07	A		
$J_{\text{meas_output}}$	2,3E-07	A		
T_{meas}	293,2	K		
$P_{\text{sme_meas}}$	6,7E-18	mol/(cm*sek*Pa(O ₂))		
$K_{\text{h_meas}}$	2260	Pa(O ₂)*dm ³ /mg		
stirring_%max_value_meas	1,00	-		
$\Delta J_{\text{stir_calwater-meas}}$	0	A	0,0E+00	0,0E+00
$\Delta J_{\text{stir_calair-meas}}$	0	A	-5,8E-23	-2,9E-23
Probe characteristics				
Type			Galvanic	
Cathode			Au	
S	0,0057	cm ²		
Anode			Pb	
Membrane			fluoroethylene-propylene (FEP)	
Electrolyte solution			KOH	
$I_{\text{sme_cal}}$	0,0013	cm		
P_{sme0}	1,01E-15	mol/(cm*sek*Pa(O ₂))		
E_{sme}	-12237	J/mol	6,0%	-367
Constants				
A_1	-139,3441		function constant	
A_2	1,58E+05		function constant	
A_3	-6,64E+07		function constant	
A_4	1,24E+10		function constant	
A_5	-8,62E+11		function constant	
B_1	11,8571		function constant	
B_2	-3840,7		function constant	
B_3	-216961		function constant	
T_0	273,15	K		
K_{h0}	636288	Pa(O ₂)*dm ³ /mg		
H	-13747	J/mol		
n	4	-		
F	96485	C/mol		
R	8,31447	J/(K*mol)		
ρ_n	101325	Pa		

*Estimation of Uncertainty in Electrochemical Amperometric Measurement of Dissolved Oxygen Concentration
Department of Chemistry, University of Tartu, Jakobi 2, 51014 Tartu, Estonia (2007)*

Input values and uncertainties for calculation

	Value	Unit	u	u/10	results
ical	20	C	0,100	0,010	%
DTinstab_water	0	C	0,015	0,002	0%
J0	0	A	0,000	0,000	1%
DJcal_output_water	0	A	0,000	0,000	0%
pcal	99700	Pa	150,000	15,000	12%
DCsaL_cal_water	0	mg/l	0,025	0,003	15%
DpCO2	0	Pa	34,895	3,490	49%
pH2O_cal	2338	Pa	117	11,690	1%
DCread_cal	0	mg/l	0,000	0,000	9%
tmeas	20	C	0,000	0,000	0%
DJmeas_output	0	A	0,000	0,000	0%
DCread_meas	0	mg/l	0,003	0,000	12%
DSme_drift_new	0	cm	0,000	0,000	1%
DSme_drift_old	0	cm	0,000	0,000	0%
DESme_drift	0	J/mol	0,000	0,000	0%
DJstir_calWater-meas	0	J/mol	0,000	0,000	0%
Esme	-12237	J/mol	-367	-36,711	0%
J_cal_water	2,27E-07	A			100%
J_meas	2,28E-07	A			
Psme_cal	6,66E-18	mol/(cm ² *sek*Pa(O2))			
Psme_meas	6,66E-18	mol/(cm ² *sek*Pa(O2))			
Kt1_cal	2260	Pa(O2)*dm3/mg			
Kt1_meas	2260	Pa(O2)*dm3/mg			
Lsme_meas	1,30E-03	cm			
W	0,98				
CsaL_cal_water	9,09	mg/l			
Cmeas	9,00	mg/l			
	0,04	u, k=1			
	0,07	U, k=2			
	0,8	%			

Appendix 3

total	DTinstab_water	J0	Dtcal_output_water	pcal	DCsat_cal_water	DpCO2	pH2O_cal	DCread_cal
20,01	0	20	20	20	20	20	20	20
	0	0,00	0	0	0	0	0	0
	0	0	1,27E-10	0	0	0	0	0
	0	0	3,10E-11	0	0	0	0	0
99700	99700	99700	99700	99715,000	99700	99700	99700	99700
	0	0	0	0	0,003	0	0	0
	0	0	0	0	0	0	3	0
2338	2338	2338	2338	2338	2338	2338	2350	2338
	0	0	0	0	0	0	0	0,000
20	20	20	20	20	20	20	20	20
	0	0	0	0	0	0	0	0
	0	0	0	0	0	0	0	0
	0	0	0	0	0	0	0	0
	0	0	0	0	0	0	0	0
	0	0	0	0	0	0	0	0
	0	0	0	0	0	0	0	0
-12237	-12237	-12237	-12237	-12237	-12237	-12237	-12237	-12237
2,27E-07	2,27E-07	2,27E-07	2,27E-07	2,27E-07	2,27E-07	2,27E-07	2,27E-07	2,27E-07
2,28E-07	2,28E-07	2,28E-07	2,28E-07	2,28E-07	2,28E-07	2,28E-07	2,28E-07	2,28E-07
6,65679E-18	6,65679E-18	6,65679E-18	6,65679E-18	6,65679E-18	6,65679E-18	6,65679E-18	6,65679E-18	6,65679E-18
6,65679E-18	6,65679E-18	6,65679E-18	6,65679E-18	6,65679E-18	6,65679E-18	6,65679E-18	6,65679E-18	6,65679E-18
2260	2260	2260	2260	2260	2260	2260	2260	2260
2260	2260	2260	2260	2260	2260	2260	2260	2260
1,30E-03	1,30E-03	1,30E-03	1,30E-03	1,30E-03	1,30E-03	1,30E-03	1,30E-03	1,30E-03
0,98	0,98	0,98	0,98	0,98	0,98	0,98	0,98	0,98
9,09	9,09	9,09	9,09	9,09	9,10	9,09	9,09	9,09
9,00	9,00	9,00	9,00	9,00	9,00	9,00	9,00	9,00
-2,5E-04	-2,7E-04	-3,2E-05	-1,2E-03	1,4E-03	2,5E-03	3,2E-03	-1,1E-03	0,0E+00
6,1E-08	7,2E-08	1,0E-09	1,5E-06	1,9E-06	6,1E-06	1,0E-06	1,2E-06	0,0E+00
total	DTinstab_water	J0	Dtcal_output_water	pcal	DCsat_cal_water	DpCO2	pH2O_cal	DCread_cal
0,5%	0,6%	0,0%	12,1%	15,3%	48,7%	0,8%	9,3%	0,0%

Instrument_IL_uncertainty

Page 4

calculation_water_calibration

Appendix 3

lmeas	DJmeas_output		DCread_meas		Dlsme_drift_new		Dlsme_drift_old		DEsme_drift		Dlsir_calwater-meas		Esme	
	20	20	20	20	20	20	20	20	20	20	20	20	20	20
2,27E-07	0	0	0	0	0	0	0	0	0	0	0	0	0	0
2,28E-07	0	0	0	0	0	0	0	0	0	0	0	0	0	0
6,65679E-18	0	0	0	0	0	0	0	0	0	0	0	0	0	0
6,65679E-18	99700	99700	99700	99700	99700	99700	99700	99700	99700	99700	99700	99700	99700	99700
2260	0	0	0	0	0	0	0	0	0	0	0	0	0	0
2260	0	0	0	0	0	0	0	0	0	0	0	0	0	0
1,30E-03	2338	2338	2338	2338	2338	2338	2338	2338	2338	2338	2338	2338	2338	2338
0,98	0	0	0	0	0	0	0	0	0	0	0	0	0	0
9,09	20,000	20	20	20	20	20	20	20	20	20	20	20	20	20
	0	0,000	0	0	0	0	0	0	0	0	0	0	0	0
	0	0	0	0,000289	0	0	0	0	0	0	0	0	0	0
	0	0	0	0	0	0	0	0	0	0	0	0	0	0
	0	0	0	0	0	0	0,000	0	0	0	0	0	0	0
	0	0	0	0	0	0	0	0,000	0	0,000	0	0	0	0
	0	0	0	0	0	0	0	0	0	0	0,000	0	0	0
	-1,2237	-1,2237	-1,2237	-1,2237	-1,2237	-1,2237	-1,2237	-1,2237	-1,2237	-1,2237	-1,2237	-1,2237	-1,2237	-1,2237
2,27E-07	2,27E-07	2,27E-07	2,27E-07	2,27E-07	2,27E-07	2,27E-07	2,27E-07	2,27E-07	2,27E-07	2,27E-07	2,27E-07	2,27E-07	2,27E-07	2,27E-07
2,28E-07	2,28E-07	2,28E-07	2,28E-07	2,28E-07	2,28E-07	2,28E-07	2,28E-07	2,28E-07	2,28E-07	2,28E-07	2,28E-07	2,28E-07	2,28E-07	2,28E-07
6,65679E-18	6,65679E-18	6,65679E-18	6,65679E-18	6,65679E-18	6,65679E-18	6,65679E-18	6,65679E-18	6,65679E-18	6,65679E-18	6,65679E-18	6,65679E-18	6,65679E-18	6,65679E-18	6,65679E-18
6,65679E-18	6,65679E-18	6,65679E-18	6,65679E-18	6,65679E-18	6,65679E-18	6,65679E-18	6,65679E-18	6,65679E-18	6,65679E-18	6,65679E-18	6,65679E-18	6,65679E-18	6,65679E-18	6,65679E-18
2260	2260	2260	2260	2260	2260	2260	2260	2260	2260	2260	2260	2260	2260	2260
2260	2260	2260	2260	2260	2260	2260	2260	2260	2260	2260	2260	2260	2260	2260
1,30E-03	1,30E-03	1,30E-03	1,30E-03	1,30E-03	1,30E-03	1,30E-03	1,30E-03	1,30E-03	1,30E-03	1,30E-03	1,30E-03	1,30E-03	1,30E-03	1,30E-03
0,98	0,98	0,98	0,98	0,98	0,98	0,98	0,98	0,98	0,98	0,98	0,98	0,98	0,98	0,98
9,09	9,09	9,09	9,09	9,09	9,09	9,09	9,09	9,09	9,09	9,09	9,09	9,09	9,09	9,09
9,00	9,00	9,00	9,00	9,00	9,00	9,00	9,00	9,00	9,00	9,00	9,00	9,00	9,00	9,00
0,0E+00	1,2E-03	2,9E-04	2,9E-04	0,0E+00	0,0E+00	0,0E+00	0,0E+00	0,0E+00	0,0E+00	0,0E+00	0,0E+00	0,0E+00	0,0E+00	diff
0,0E+00	1,5E-06	8,3E-08	8,3E-08	0,0E+00	0,0E+00	0,0E+00	0,0E+00	0,0E+00	0,0E+00	0,0E+00	0,0E+00	0,0E+00	0,0E+00	diff#2
														1,3E-05 sum(diff#2)
0,0%	DJmeas_output	12,1%	DCread_meas	0,7%	Dlsme_drift_new	0,0%	Dlsme_drift_old	0,0%	DEsme_drift	0,0%	Dlsir_calwater-meas	Esme	index	100,0% sum(index)

Instrument_II_uncertainty

Page 5

calculation_water_calibration

Input values and uncertaintys for calculation

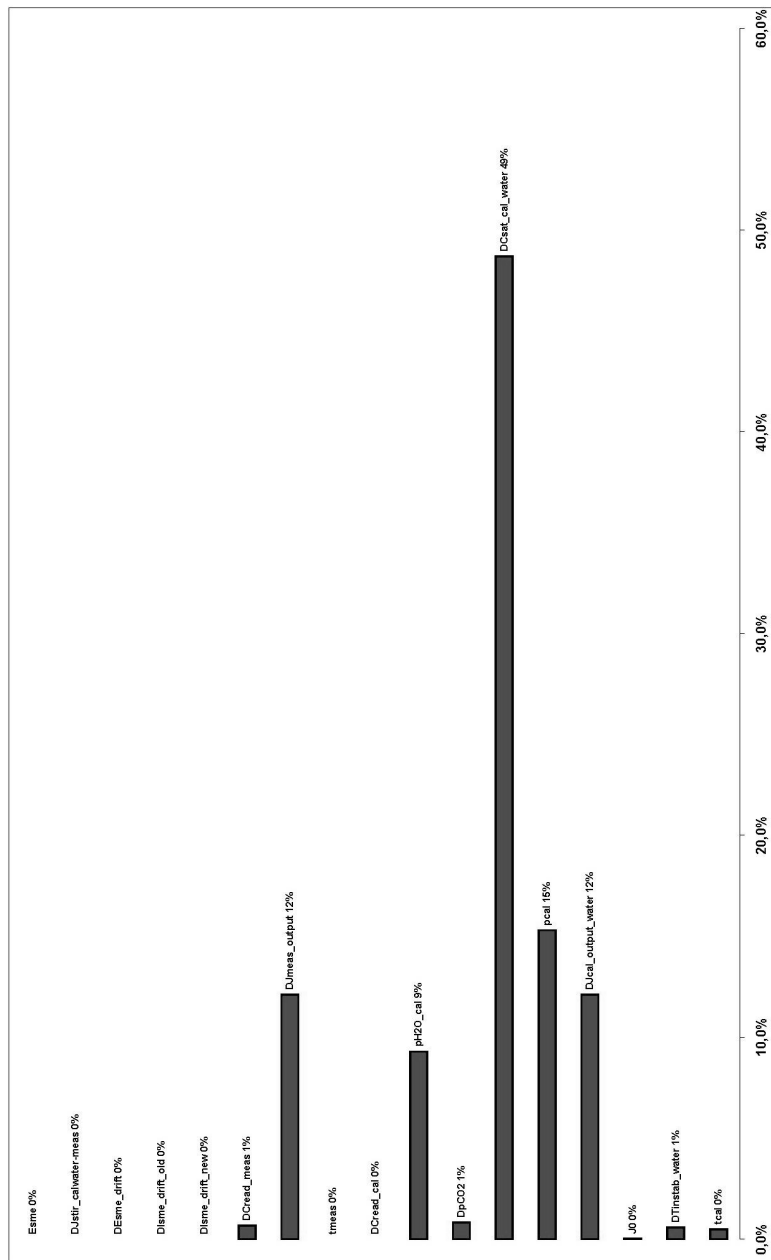
	Value	Unit	u	u/10	results
ical	20	C	0,100	0,010	%
DTinstab_air	0	C	0,100	0,010	0%
J0	0	A	0,000	0,000	22%
Ducal_output_air	0	A	0,000	0,000	0%
pcal	99700	Pa	150,000	15,000	1%
DCsat_cal_water	0	mg/l	0,025	0,003	13%
DpCO2	0	Pa	34,895	3,490	43%
pH2O_cal	2338	Pa	117	11,690	1%
Dcread_cal	0	mg/l	0,000	0,000	8%
g	1,017	-	0,000	0,000	0%
tmeas	20	C	0,000	0,000	0%
Dumeas_output	0	A	0,000	0,000	0%
Dcread_meas	0	mg/l	0,003	0,000	11%
Disme_drift_new	0	cm	0,000	0,000	1%
Disme_drift_old	0	cm	0,000	0,000	0%
Desme_drift	0	J/mol	0,000	0,000	0%
Dlslir_calair-meas	0	A	0,000	0,000	0%
Esme	-12237	J/mol	-367	-36,711	0%
J_cal_air	2,30E-07	A			100%
J_meas	2,28E-07	A			
Psme_cal	6,66E-18	mol/(cm²*sek)*Pa(O2)			
Psme_meas	6,66E-18	mol/(cm²*sek)*Pa(O2)			
Kt_cal	2260	Pa(O2)*dm3/mg			
Kt_meas	2260	Pa(O2)*dm3/mg			
L_sme_meas	1,30E-03	cm			
W	0,98				
Csat_cal_air	9,09	mg/l			
Cmeas	9,00	mg/l			
	0,04	u, k=1			
	0,08	U, k=2			
	0,8	%			

[illegible]

calculation_air_calibration

Instrument_II_uncertainty

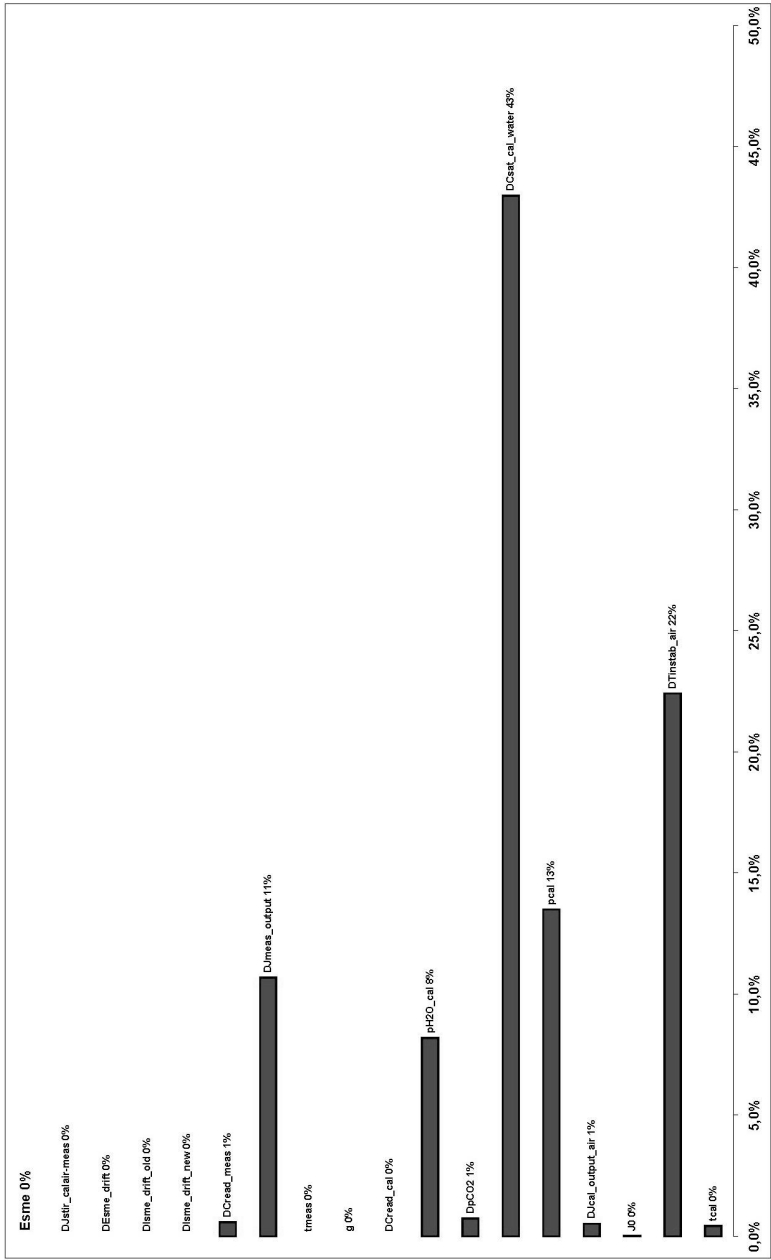
Appendix 3



Instrument_II_uncertainty

Page 9

uncertainty_budget_water



Instrument_II_uncertainty

Page 10

uncertainty_budget_air

PUBLICATIONS

Reproduced with kind permission of Springer Science and Business Media from
Accreditation and Quality Assurance, 2004, vol. 9
L. Jalukse, I. Leito, A. Mashirin and T. Tenno,
Estimation of uncertainty in electrochemical amperometric measurement
of dissolved oxygen concentration
Pages 340–348
<http://dx.doi.org/10.1007/s00769-004-0783-4>

Copyright 2007 Springer Science and Business Media

Reproduced with permission from Measurement Science and Technology,
2007, vol. 18
L. Jalukse and I. Leito
Model-based measurement uncertainty estimation
in amperometric dissolved oxygen concentration measurement.
Pages 1877–1886
<http://dx.doi.org/10.1088/0957-0233/18/7/013>

Copyright 2007 IOP Publishing Limited
<http://journals.iop.org/>

Reproduced with kind permission of Springer Science and Business Media from
Accreditation and Quality Assurance, 2006, vol. 10
L. Jalukse, V. Vabson and I. Leito,
In situ interlaboratory comparisons for dissolved oxygen concentration and pH.
Pages 562–564
<http://dx.doi.org/10.1007/s00769-005-0058-8>

Copyright 2007 Springer Science and Business Media

CURRICULUM VITAE

Lauri Jalukse

Born: December 05, 1978, Rapla, Estonia
Citizenship: Estonian
Marital status: Committed
Address: Institute of Chemical Physics
University of Tartu
2 Jakobi Street, Tartu 51014, Estonia
Phone: +372 55518440
E-mail: lauri.jalukse@ut.ee

Education

- 1997–2001 Department of Chemistry, University of Tartu, Estonia; B.Sc. (chemistry) 2001
2001–2003 Department of Chemistry, University of Tartu, Estonia, M.Sc. (physical and analytical chemistry) 2003
2003– Department of Chemistry, University of Tartu, Estonia, Ph.D. student, doctoral advisor prof. Ivo Leito (Ph.D)

Professional employment and retraining

- 2005– University of Tartu, Institute of Chemical Physics, research fellow
2005– Doctoral School of Materials Science and Technology, extraordinary researcher

Main scientific publications

1. **L. Jalukse**, E. Koort, J. Traks and I. Leito, GUM Workbench as measurement modelling and uncertainty estimation software: experience at University of Tartu. *Accred. Qual. Assur.* 2003, 8, 520–522, <http://dx.doi.org/10.1007/s00769-003-0663-3>
2. **L. Jalukse**, I. Leito, A. Mashirin and T. Tenno, Estimation of uncertainty in electrochemical amperometric measurement of dissolved oxygen concentration. *Accreditation and Quality Assurance* 2004, 9, 340–348, <http://dx.doi.org/10.1007/s00769-004-0783-4>
3. A. Rodima, M. Vilbaste, O. Saks, E. Jakobson, E. Koort, V. Pihl, L. Sooväli, **L. Jalukse**, J. Traks, K. Virro, H. Annuk, K. Aruoja, A. Floren, E. Indermitte, M. Jürgenson, P. Kaleva, K. Kepler and I. Leito, ISO 17025 quality system in a university environment. *Accreditation and Quality Assurance*, 2005, 10, 369–372 <http://dx.doi.org/10.1007/s00769-005-0011-x>
4. **L. Jalukse**, V. Vabson and I. Leito, In situ interlaboratory comparisons for dissolved oxygen concentration and pH. *Accreditation and Quality Assurance* 2006, 10, 562–564, <http://dx.doi.org/10.1007/s00769-005-0058-8>
5. **L. Jalukse** and I. Leito, Model-based measurement uncertainty estimation in amperometric dissolved oxygen concentration measurement. *Measurement Science and Technology*, 2007, 18, 1877–1886, <http://dx.doi.org/10.1007/s00769-005-0058-8>

CURRICULUM VITAE

Lauri Jalukse

Sündinud: 05. detsember, 1978, Rapla, Eesti
Kodakondsus: Eesti
Perekonnaseis: vabaabielu
Aadress: Keemilise füüsika instituut
Tartu Ülikool
Jakobi 2, Tartu 51014, Eesti
Telefon: +372 55518440
E-mail: lauri.jalukse@ut.ee

Haridus

1997–2001 Tartu Ülikooli keemiaosakonna üliõpilane; *B.Sc.* (keemia) 2001
2001–2003 Tartu Ülikooli keemiaosakonna üliõpilane; *M.Sc.* (keemia) 2003
2003– Tartu Ülikooli keemiaosakonna doktorant, juhendaja prof. Ivo Leito

Teenistuskäik

2005– Tartu Ülikooli Keemilise füüsika instituudi teadur
2005– Materjaliteaduse ja materjalide tehnoloogia erakorraline teadur

Tähtsamad teaduspublikatsioonid

1. **L. Jalukse**, E. Koort, J. Traks and I. Leito, GUM Workbench as measurement modelling and uncertainty estimation software: experience at University of Tartu. *Accred. Qual. Assur.* 2003, 8, 520–522, <http://dx.doi.org/10.1007/s00769-003-0663-3>
2. **L. Jalukse**, I. Leito, A. Mashirin and T. Tenno, Estimation of uncertainty in electrochemical amperometric measurement of dissolved oxygen concentration. *Accreditation and Quality Assurance* 2004, 9, 340–348, <http://dx.doi.org/10.1007/s00769-004-0783-4>
3. A. Rodima, M. Vilbaste, O. Saks, E. Jakobson, E. Koort, V. Pihl, L. Sooväli, **L. Jalukse**, J. Traks, K. Virro, H. Annuk, K. Aruoja, A. Floren, E. Indermitte, M. Jürgenson, P. Kaleva, K. Kepler and I. Leito, ISO 17025 quality system in a university environment. *Accreditation and Quality Assurance*, 2005, 10, 369–372 <http://dx.doi.org/10.1007/s00769-005-0011-x>
4. **L. Jalukse**, V. Vabson and I. Leito, In situ interlaboratory comparisons for dissolved oxygen concentration and pH. *Accreditation and Quality Assurance* 2006, 10, 562–564, <http://dx.doi.org/10.1007/s00769-005-0058-8>
5. **L. Jalukse** and I. Leito, Model-based measurement uncertainty estimation in amperometric dissolved oxygen concentration measurement. *Measurement Science and Technology*, 2007, 18, 1877–1886, <http://dx.doi.org/10.1007/s00769-005-0058-8>

DISSERTATIONES CHIMICAE UNIVERSITATIS TARTUENSIS

1. **Toomas Tamm.** Quantum-chemical simulation of solvent effects. Tartu, 1993, 110 p.
2. **Peeter Burk.** Theoretical study of gas-phase acid-base equilibria. Tartu, 1994, 96 p.
3. **Victor Lobanov.** Quantitative structure-property relationships in large descriptor spaces. Tartu, 1995, 135 p.
4. **Vahur Mäemets.** The ^{17}O and ^1H nuclear magnetic resonance study of H_2O in individual solvents and its charged clusters in aqueous solutions of electrolytes. Tartu, 1997, 140 p.
5. **Andrus Metsala.** Microcanonical rate constant in nonequilibrium distribution of vibrational energy and in restricted intramolecular vibrational energy redistribution on the basis of Slater's theory of unimolecular reactions. Tartu, 1997, 150 p.
6. **Uko Maran.** Quantum-mechanical study of potential energy surfaces in different environments. Tartu, 1997, 137 p.
7. **Alar Jänes.** Adsorption of organic compounds on antimony, bismuth and cadmium electrodes. Tartu, 1998, 219 p.
8. **Kaido Tammeveski.** Oxygen electroreduction on thin platinum films and the electrochemical detection of superoxide anion. Tartu, 1998, 139 p.
9. **Ivo Leito.** Studies of Brønsted acid-base equilibria in water and non-aqueous media. Tartu, 1998, 101 p.
10. **Jaan Leis.** Conformational dynamics and equilibria in amides. Tartu, 1998, 131 p.
11. **Toonika Rinken.** The modelling of amperometric biosensors based on oxidoreductases. Tartu, 2000, 108 p.
12. **Dmitri Panov.** Partially solvated Grignard reagents. Tartu, 2000, 64 p.
13. **Kaja Orupõld.** Treatment and analysis of phenolic wastewater with micro-organisms. Tartu, 2000, 123 p.
14. **Jüri Ivask.** Ion Chromatographic determination of major anions and cations in polar ice core. Tartu, 2000, 85 p.
15. **Lauri Vares.** Stereoselective Synthesis of Tetrahydrofuran and Tetrahydropyran Derivatives by Use of Asymmetric Horner-Wadsworth-Emmons and Ring Closure Reactions. Tartu, 2000, 184 p.
16. **Martin Lepiku.** Kinetic aspects of dopamine D_2 receptor interactions with specific ligands. Tartu, 2000, 81 p.
17. **Katrin Sak.** Some aspects of ligand specificity of P2Y receptors. Tartu, 2000, 106 p.
18. **Vello Pällin.** The role of solvation in the formation of iotsitch complexes. Tartu, 2001, 95 p.

19. **Katrin Kollist.** Interactions between polycyclic aromatic compounds and humic substances. Tartu, 2001, 93 p.
20. **Ivar Koppel.** Quantum chemical study of acidity of strong and superstrong Brønsted acids. Tartu, 2001, 104 p.
21. **Viljar Pihl.** The study of the substituent and solvent effects on the acidity of OH and CH acids. Tartu, 2001, 132 p.
22. **Natalia Palm.** Specification of the minimum, sufficient and significant set of descriptors for general description of solvent effects. Tartu, 2001, 134 p.
23. **Sulev Sild.** QSPR/QSAR approaches for complex molecular systems. Tartu, 2001, 134 p.
24. **Ruslan Petrukhin.** Industrial applications of the quantitative structure-property relationships. Tartu, 2001, 162 p.
25. **Boris V. Rogovoy.** Synthesis of (benzotriazolyl)carboximidamides and their application in relations with *N*- and *S*-nucleophiles. Tartu, 2002, 84 p.
26. **Koit Herodes.** Solvent effects on UV-vis absorption spectra of some solvatochromic substances in binary solvent mixtures: the preferential solvation model. Tartu, 2002, 102 p.
27. **Anti Perkson.** Synthesis and characterisation of nanostructured carbon. Tartu, 2002, 152 p.
28. **Ivari Kaljurand.** Self-consistent acidity scales of neutral and cationic Brønsted acids in acetonitrile and tetrahydrofuran. Tartu, 2003, 108 p.
29. **Karmen Lust.** Adsorption of anions on bismuth single crystal electrodes. Tartu, 2003, 128 p.
30. **Mare Piirsalu.** Substituent, temperature and solvent effects on the alkaline hydrolysis of substituted phenyl and alkyl esters of benzoic acid. Tartu, 2003, 156 p.
31. **Meeri Sassian.** Reactions of partially solvated Grignard reagents. Tartu, 2003, 78 p.
32. **Tarmo Tamm.** Quantum chemical modelling of polypyrrole. Tartu, 2003. 100 p.
33. **Erik Teinemaa.** The environmental fate of the particulate matter and organic pollutants from an oil shale power plant. Tartu, 2003. 102 p.
34. **Jaana Tammiku-Taul.** Quantum chemical study of the properties of Grignard reagents. Tartu, 2003. 120 p.
35. **Andre Lomaka.** Biomedical applications of predictive computational chemistry. Tartu, 2003. 132 p.
36. **Kostyantyn Kirichenko.** Benzotriazole — Mediated Carbon–Carbon Bond Formation. Tartu, 2003. 132 p.
37. **Gunnar Nurk.** Adsorption kinetics of some organic compounds on bismuth single crystal electrodes. Tartu, 2003, 170 p.
38. **Mati Arulepp.** Electrochemical characteristics of porous carbon materials and electrical double layer capacitors. Tartu, 2003, 196 p.

39. **Dan Cornel Fara.** QSPR modeling of complexation and distribution of organic compounds. Tartu, 2004, 126 p.
40. **Riina Mahlapuu.** Signalling of galanin and amyloid precursor protein through adenylate cyclase. Tartu, 2004, 124 p.
41. **Mihkel Kerikmäe.** Some luminescent materials for dosimetric applications and physical research. Tartu, 2004, 143 p.
42. **Jaanus Kruusma.** Determination of some important trace metal ions in human blood. Tartu, 2004, 115 p.
43. **Urmas Johanson.** Investigations of the electrochemical properties of polypyrrole modified electrodes. Tartu, 2004, 91 p.
44. **Kaido Sillar.** Computational study of the acid sites in zeolite ZSM-5. Tartu, 2004, 80 p.
45. **Aldo Oras.** Kinetic aspects of dATP α S interaction with P2Y₁ receptor. Tartu, 2004, 75 p.
46. **Erik Mölder.** Measurement of the oxygen mass transfer through the air-water interface. Tartu, 2005, 73 p.
47. **Thomas Thomberg.** The kinetics of electroreduction of peroxodisulfate anion on cadmium (0001) single crystal electrode. Tartu, 2005, 95 p.
48. **Olavi Loog.** Aspects of condensations of carbonyl compounds and their imine analogues. Tartu, 2005, 83 p.
49. **Siim Salmar.** Effect of ultrasound on ester hydrolysis in aqueous ethanol. Tartu, 2006, 73 p.
50. **Ain Uustare.** Modulation of signal transduction of heptahelical receptors by other receptors and G proteins. Tartu, 2006, 121 p.
51. **Sergei Yurchenko.** Determination of some carcinogenic contaminants in food. Tartu, 2006, 143 p.
52. **Kaido Tamm.** QSPR modeling of some properties of organic compounds. Tartu, 2006, 67 p.
53. **Olga Tšubrik.** New methods in the synthesis of multisubstituted hydrazines. Tartu. 2006, 183 p.
54. **Lilli Sooväli.** Spectrophotometric measurements and their uncertainty in chemical analysis and dissociation constant measurements. Tartu, 2006, 125 p.
55. **Eve Koort.** Uncertainty estimation of potentiometrically measured pH and pK_a values. Tartu, 2006, 139 p.
56. **Sergei Kopanchuk.** Regulation of ligand binding to melanocortin receptor subtypes. Tartu, 2006, 119 p.
57. **Silvar Kallip.** Surface structure of some bismuth and antimony single crystal electrodes. Tartu, 2006, 107 p.
58. **Kristjan Saal.** Surface silanization and its application in biomolecule coupling. Tartu, 2006, 77 p.
59. **Tanel Tätte.** High viscosity Sn(OBu)₄ oligomeric concentrates and their applications in technology. Tartu, 2006, 91 p.

60. **Dimitar Atanasov Dobchev.** Robust QSAR methods for the prediction of properties from molecular structure. Tartu, 2006, 118 p.
61. **Hannes Hagu.** Impact of ultrasound on hydrophobic interactions in solutions. Tartu, 2007, 81 p.
62. **Rutha Jäger.** Electroreduction of peroxodisulfate anion on bismuth electrodes. Tartu, 2007, 142 p.
63. **Kaido Viht.** Immobilizable bisubstrate-analogue inhibitors of basophilic protein kinases: development and application in biosensors. Tartu, 2007, 88 p.
64. **Eva-Ingrid Rõõm.** Acid-base equilibria in nonpolar media. Tartu, 2007, 156 p.
65. **Sven Tamp.** DFT study of the cesium cation containing complexes relevant to the cesium cation binding by the humic acids. Tartu, 2007, 102 p.
66. **Jaak Nerut.** Electroreduction of hexacyanoferrate(III) anion on Cadmium (0001) single crystal electrode. Tartu, 2007, 180 p.